# SEGMENTATION OF HIGH-RESOLUTION SATELLITE IMAGERY USING A HYBRIDIZATION OF COLOUR-BASED AND K-MEANS CLUSTERING TECHNIQUES FOR RESCUE MISSION

**BY**

**AGBO, Christopher**
**M.TECH/SICT/2019/9853**

**DEPARTMENT OF COMPUTER SCIENCE**
**FEDERAL UNIVERSITY OF TECHNOLOGY**
**MINNA**

**JULY, 2023**

# SEGMENTATION OF HIGH-RESOLUTION SATELLITE IMAGERY USING A HYBRIDIZATION OF COLOUR-BASED AND K-MEANS CLUSTERING TECHNIQUES FOR RESCUE MISSION

**BY**

**AGBO, Christopher**
**M.TECH/SICT/2019/9853**

**A THESIS SUBMITTED TO THE POSTGRADUATE SCHOOL FEDERAL UNIVERSITY OF TECHNOLOGY, MINNA, NIGERIA IN PARTIAL FULFILMENT OF THE REQUIRMENTS FOR THE AWARD OF THE DEGREE OF MASTER OF TECHNOLOGY IN COMPUTER SCIENCE.**

**JULY, 2023**

**ABSTRACT**

Rapid response to natural disasters, like floods, is essential to reducing casualties and suffering. Rescue teams must have quick access to reliable data. Satellite imagery offers a lot of information that can be analysed to help identify disaster-affected areas. In order to detect and manage natural disasters, segmentation analysis of satellite images is becoming an increasingly crucial component of environmental and climatic monitoring. Image segmentation, which separates a single image into several homogeneous fragments, enhances pattern recognition. Object placement, lighting, shadow, and other factors can all affect how effective an image segmentation technique is. There is no one method that can be used to segment all imagery, although some strategies have been more successful than others. Individual segmentation techniques have flaws like region rising, initial seed selection, noise and low intensity transition, but combining two or more techniques reduces these flaws and boosts segmentation accuracy. This study proposes a method for flooded area identification and segmentation based on a combination of colour-based and k-mean clustering (KC) segmentation techniques. When comparing the proposed technique (colour-based KC model) with commonly used segmentation techniques like Colour thresholding (CT), Region-based Active Contour (RAC) and Edge-based Active Contour (EAC) segmentation, the proposed method achieved better performance metrics with a 0.8234 Jaccard Index, 0.9234 Dice similarity coefficient, 0.9589 precision, 0.9078 recall and 0.9327 BFscore, which was higher than the other four segmentation techniques and previous works. The results obtained indicated that the proposed technique performed better than existing techniques in detecting and segmenting flooded areas in satellite images. Future work can explore other segmentation methods and test the analysed techniques on diverse satellite images with varying scenarios.

## TABLE OF CONTENT

## LIST OF TABLES

## LIST OF FIGURES

# CHAPTER ONE

# 1.0 INTRODUCTION

## 1.1 Background to the Study

Digital photographs are being used in many different scientific disciplines.The existence of very powerful image processing methods has made digital images useful in different applications and has led to the development of various approaches to digital image analysis in the last few decades. Digital image processing techniques can enhance the picture analysis process and be used to find details that are not always obvious to the human eye, enabling significant advancement in a number of sectors. Besides improvements in the analysis, the process is usually much faster than an expert's manual analysis. Scientific fields that are using digital images are numerous: security, agriculture, astronomy, medicine, education, disaster management, and finance (CaporHrosik *et al.*, 2019).

Image segmentation (IS) is presently one of the key tasks in the field of image processing (Soomro *et al.*, 2018). IS is a technique that splits an image into meaningful chunks with related characteristics, features, and descriptors. It is used to identify objects and edges in images, such as lines and geometric. This means that each pixel in a picture is given a name so that all of the labels for that pixels have the same visual properties. By condensing an image's information into meaningful ways, segmentation primarily aims to make the image's representation understandable (Kaur and Goyal, 2013). IS is crucial for a variety of industries, including satellite imaging, therapeutic diagnosis, and others (Sathya and Malathi, 2011). Diverse techniques have been suggested and presented for image segmentation. In general, the most common approaches are Edge-based technique, histogram-based method, Region-based approach, and Clustering-based segmentation. Satellite image obtained from remote

sensing plays a vital role in providing quantitative and qualitative geographical information (Fawwaz *et al.*, 2018). The wealth of valuable information that is generated from the satellite images has tremendously benefitted and boosted many scientific research and applications depending on the required studies such as, land surface mapping and monitoring, research academia, climate change investigation, ecosystem dynamics monitoring, city planning, archaeological investigations, government, and national security (Sathya and Malathi, 2011; Ulmas and Liiv, 2020).

The study of natural disaster imagery and disaster management are two areas where the use of satellite photography has become crucial to preparation (Park and Lee, 2019). The amount, speed, and accessibility of satellite imagery covering a particular chaotic situation or disaster occurrence has significantly increased when compared to the situation roughly ten years ago (Amit *et al.*, 2016). Prioritizing rescue missions, disaster response, and coordinating relief activities are crucial after a disaster. Since resources are frequently scarce in disaster-affected areas, these must be carried out quickly and effectively, and it is crucial to pinpoint the places that have sustained the most damage (Kaku, 2019). The most frequent natural calamity that impacts people each year all across the globe is flooding (Zhang *et al.*, 2020). Most of the time, it directly affects human life and causes property damage. Many strategies have been developed in recent years to coordinate rescue activities in such situations in a more effective manner (Muhadi *et al.*, 2020). In order to track floods and undertake appropriate risk analysis, much study has been undertaken in the area of monitoring floods using satellite pictures.

A crucial step in visual sensor devices is image processing, which is the use of computational models to extract valuable information from digital images (Geetha *et al.*, 2017). IS, which divides an image into a number of regions sometimes depending on the characteristics of its pixels, is frequently used to interpret the image content. IS has been

used, particularly, in the areas of water management, autonomous driving, and diagnostic imaging (Bhadoria *et al.*, 2020). IS may entail separating the foreground (in this case, the water characteristics) from the background in flood disaster scenarios. Scientists and business presently employ a variety of IS methods, including thresholding, boundary-based, region-based, and hybrid methods (Johnson and Ma, 2020).

In general, the selection of features in IS algorithms is important. According to Nath and Deb (2010), colour information is one of the most intriguing aspects of digital photographs. Information about texture or pattern is another aspect that is frequently employed. These key characteristics were widely employed by researchers to locate flood episodes. Lai *et al.* (2007) used threshold values to identify probable foreground zones to detect flooding events. Geetha *et al.* (2017) used crowd-sourced pictures and a Colour-based separation threshold to determine the size of flood areas. The effectiveness of three various image processing methods for flood monitoring systems was assessed by Qianyu *et al.* (2018). According to their testing findings, the canny edge detection method had a high level of success in locating the flooded area. Popescu *et al*. (2018) utilized the generative adversarial networks (GAN) for flooded area segmentation. The performance of the GAN network was tested on 60 images. Several techniques have been developed to enhance segmentation accuracy from the literature reviews. However, different IS techniques work better for certain scenarios and image kinds. In this study, a hybrid technique that combines Colour-based and k-means clustering is presented to improve segmentation outcomes for various image types, particularly in the flood scenario.

## 1.2 Problem Statement

It can be challenging to separate a satellite image into various classes or regions with varying textures. Typically, it is unknown beforehand what kinds of textures, how many textures, and which regions include which textures exist in a satellite image. Different segmentation approaches, such as edge-based, region-based, watershed-based, and clustering segmentation techniques, can be used to complete the segmentation and monitoring task. Region-based segmentation performs a comparable function based on the uniformity of a desired feature within a sub-region, as opposed to edge-based segmentation, which divides a picture based on discontinuities with sub-regions (Hernández *et al.,* 2022). Only images with distinct intensity transitions and low noise levels typically lend themselves to edge-based segmentation by gradient operation. Different smoothing operations are frequently necessary as preprocessing because of its sensitivity to noise, and the smoothing effect as a result blurs the edge information. The region-based procedures are hampered by region rising, initial seed selection, and appropriate qualities for growing the regions. The under-segmentation issue affects the watershed segmentation method (Kenneth *et al.,* 2019). The edge-based is not suitable for segmentation of flooded area segmentation because the satellite imageries are noisy and have low intensity transition. Region-based technique relies on examining and joining neighbouring pixels to a region class of no edges, which makes it unsuitable for the flooded area problem because flooded areas are sometimes separated by edges. A distinguishing feature of flooded area satellites imagery is the Colour of the affected area. The flooded areas are mostly brownish in Colour, and this makes segmentation based on Colour suitable. In the case of colour-based segmentation the object edges are not required to be sharp or free of noise and it does the not require that the object of interest have no edges separating them as in the case of region-based technique. In order

to decrease the computational cost by averting feature calculation for every pixel in the image the colour-based segmentation is combined with k-means clustering.

## 1.3 Aim and Objectives

The aim of this thesis is to develop a hybridised image segmentation technique based on a combination of colour thresholding and K-means clustering that can be used in disaster management.

The objectives of this study are:

i. To collect flood satellite images dataset from Airbus Intelligence, NASA Earth Observatory and Maxar Open Data Program.
ii. To hybridise both image segmentation techniques (Colour threshold-based and K-means clustering) for flood detection in satellite imagery.
iii. To evaluate the performance of the technique in (ii) using precision, recall, Intersection-over-Union, Boundary F1 Score and dice similarity coefficient.

## 1.4 Scope of the Study

This research focuses on automatic flooded area detection and segmentation using a combination of Colour-based and K-means clustering segmentation techniques and focused on the performance of other single methods like edge-based, and region-based techniques. However, this study did not consider the effect of combining other image segmentation techniques. There are several natural disasters which require effective management such as wildfire, earthquake, drought, and hurricane but this research focused on just the flooding natural disaster.

## 1.5 Significance of the Study

By combining colour thresholding and k-means clustering techniques, the strengths of both methods are taken to achieve more accurate and robust image segmentation. As the

colour thresholding technique was used to extract the main colours in the image, while k-means clustering can be used to group similar pixels together based on their colour values. The significance of this study lies in its potential to improve the accuracy and efficiency of image segmentation in various computer vision applications. By combining these techniques, we can achieve more precise segmentation of complex images, leading to better results in downstream applications.

The hybridization of colour thresholding and k-means clustering for image segmentation has the potential to benefit a wide range of industries and applications that rely on accurate and efficient image analysis such as medical imaging, robotics and autonomous systems, agriculture, industrial inspection and entertainment.

Furthermore, researchers would benefit from this study as it gives insight on existing algorithms on disaster detection and segmentation thus enhancing the decision-making process towards selecting the appropriate detection and segmentation technique to implement or to modify towards natural disaster management.

## 1.6 Organization of the Thesis

The five segments that make up this study project range in number from Chapter 1 to Chapter 5. The first chapter discusses the study's historical context. It comprises of the problem statement, the aim and objectives, the scope of the investigation, and the study's importance. In chapter two, a survey of earlier related literature is offered. Chapter three introduces the research approach. This includes segmentation methods for flooded areas. The details of the actual experimentation are detailed in Chapter 4, along with a comparison of the findings to those of earlier approaches. In chapter five, conclusions and recommendations for further study were presented.

# CHAPTER TWO

# 2.0 LITERATURE REVIEW

## 2.1 Overview of Natural Disaster Management

Regardless of any other apparent contributing elements, a disaster is marked by unusual, life-threatening physical destruction that is ascribed to the natural forces (Yu *et al.*, 2018). Disasters can be categorised as either natural or man-made (technical). Natural disasters include events brought on by geophysical, hydrologic, atmospheric, biological, extraterrestrial, or climatic factors risks (Manfré *et al.*, 2012). These comprise incidents resulting from dangers including earthquakes, tsunamis, storms, and floods. Disasters that are not brought on by natural occurrences, such as technology catastrophes and terrorist attacks, are referred to as man-made disasters (Celik and Corbacioglu, 2010).

Natural disasters frequently have catastrophic effects and long-lasting ramifications on society, economies, and humanity. 330 natural disasters were reported to have occurred in the world in 2013, resulting in more than 21,610 fatalities, 96.5 million victims, and $118.6 billion in damages (Guha-Sapir *et al.,* 2015). Hurricane Katrina, which hit the U.S. Gulf Coast on August 29, 2005, is proof that even isolated incidents can result in extensive harm (Knabb *et al.,* 2005). Hurricane Katrina caused over 1,800 fatalities, flooding and structural damage to 2.5 million homes, the eviction of about 1.2 million people, and economic effects that could reach $300 billion (Brunsma *et al.*, 2010). Another instance of a single event causing extensive destruction was the magnitude 7.0 earthquake that struck Haiti on January 12, 2010. More than 230,000 people perished, making an earthquake of magnitude 7.0 twice as deadly as any other (Bilham, 2010). Port-au-Prince, the capital of Haiti, experienced severe losses, with 15% of the population more than 2.5 million people either dead or injured and 1.5 million people without a place to live (Bilham, 2010). The earthquake's devastation is believed to have

caused financial damage of around $8.1 billion (Cavallo *et al.,* 2010). Effective procedures for disaster management are essential since natural disasters result in enormous losses. The body of policy and procedural choices, operational activities, players, and technology that are relevant to the different phases of a disaster at all levels is known as disaster management (Lettieri *et al.,* 2009). The many phases of disaster management comprise (Seaberg *et al.,* 2017):

i. **Mitigation**: A disaster's risk of occurring or the amount of damage it causes can both be reduced through mitigation. Resource allotment, defence spending, risk management, and climate forecasting are examples of mitigation efforts (Khan *et al.,* 2020).

ii. **Preparedness:** Activities that improve the possibility of an effective catastrophe response are preparedness. Activities that foresee calamities include resource extraction, insurance investment, resource hoarding, and resource protection.

iii. **Response:** Actions taken right away after a calamity in an effort to lessen the harm done. Response actions include things like medical aid, evacuations, and search and rescue operations.

iv. **Recovery:** Activities that assist the disaster-affected population in getting back to normal. Activities during the recovery phase would include developing temporary housing, providing financial aid, removing debris, and undertaking rebuilding projects (Sun *et al.,* 2020).

Disaster management is a subject researched throughout many fields due to the dynamic nature of catastrophes and the unpredictability in handling them, allowing emergency responders and everyone else involved in emergency to successfully plan for and react to them. The four components of disaster mitigation are outlined above, and disaster

management is the coordination of resources and responsibilities across each of them (Westen, 2000).

Digital IS is a useful tool to investigate since disaster management requires strategic interactions among multiple decision-makers, levels of government, the commercial sector, and nonprofit groups. Image segmentation is a productive approach to identify the disaster zones in order to respond to emergencies effectively.

## 2.2 Image Segmentation (IS)

IS is the process of dividing a digital image into various image segments, sometimes referred to as image regions or image objects (sets of pixels), in digital image processing and computer vision (Yuheng and Hao, 2017). The purpose of segmentation is to reduce complexity and transform an image into something more relevant and understandable. Typically, IS is used to identify objects and borders like lines, and curves in images (Zaitoun and Aqel, 2015). IS, more properly, is the process of giving each pixel in an image a label so that pixels with the same label have certain properties (Cheng *et al.*, 2001; Liu *et al.*, 2019).

A set of segments that together encompass the full image, or a set of contours taken from the image, are the products of IS. Regarding any characteristic or computed feature, such as colour, intensity, or texture, every pixel in a zone is comparable (Kang *et al.*, 2009; Udupa *et al.*, 2006).

Image segmentation is an important task in many computer vision applications, including object detection and recognition, image editing, medical image analysis, and autonomous driving. It is a challenging task, as images can be complex and contain noise, occlusions, and other types of variations. Therefore, a combination of different segmentation techniques or a hybrid approach may be used to achieve the best results.

### 2.2.1 Application of image segmentation

Image Segmentation has many areas of applications such as in content-based image retrieval, machine vision and also in medical imaging. Following are a few examples of how image segmentation is used in practise:

#### 2.2.1.1 Content-based image retrieval

The process of applying computer vision techniques to the issue of finding digital photographs in huge datasets is known as content-based image retrieval (Latif *et al.*, 2019). "Content-based" refers to a search that examines the image content rather than its associated metadata, such as its keywords, tags, or descriptions. Colours, forms, textures, or any other information that can be inferred from the image itself may be referred to as "content" in this sense (Hameed *et al.*, 2021). Content-based picture retrieval is preferred since searches that just employ metadata depend on the accuracy and completeness of the annotations (Patel and Yerpude, 2018).

#### 2.2.1.2 Machine vision

The ability of a computer to comprehend the world is known as machine vision. Contrary to image processing, which produces another image, machine vision uses technology and methodologies to automatically extract information from images (Patel *et al.*, 2012). A basic signal or a more complicated set of data, such as the identification, location, and orientation of each object in a picture, can be used as the information that is retrieved (Patel *et al.*, 2013). The data can be applied to robotic and process navigation, automatic examination, video surveillance, and vehicle guidance, among other things (Robie *et al.*, 2017).

#### 2.2.1.3 Computer graphics

Applications like virtual reality and augmented reality are made possible by the use of image segmentation in computer graphics, which allows items to be extracted from an image or video and superimposed onto a new background. (Freeman *et al.*, 2017).

#### 2.2.1.4 Medical imaging

Medical imaging is a technique and a procedure that involves taking pictures of the inside of a person for clinical evaluation, medical intervention, and to show how certain organs or tissues are functioning (physiology) (Kaissis *et al.*, 2020; Suzuki, 2017). Medical imaging aims to identify and cure disease by detecting interior structures concealed by the skin and bones (Zhou *et al.*, 2021). In order to detect anomalies, medical imaging also creates a database of typical anatomy and physiology. It is possible to find cancers and other illnesses using medical imaging (Wu *et al.*, 2013), tissue volume measurements (Ye *et al.*, 2022), analysis of anatomical structure (Kamalakannan *et al.*, 2010) and Surgery preparation.

#### 2.2.1.5 Video compression

In order to enable more effective video compression and transmission, image segmentation can be utilised to divide a video stream into smaller segments depending on motion or scene changes (Sengar & Mukhopadhyay, 2020; F. Zhang & Bull, 2011).

#### 2.2.1.6 Object detection and tracking

Identifying occurrences of semantic items of a specific class (such as people, houses, or vehicles) in digital photos and videos is the task of object detection, a branch of computer vision applications (Wang *et al.*, 2022; Zhao *et al.*, 2019). Face detection is one of the well-researched object detection fields (Khan *et al.*, 2019; Kumar *et al.*,

2018) and detection of pedestrians (Amato *et al.,* 2019; Jiang *et al.,* 2019; Z. Yi *et al.,* 2019; S. Zhang *et al*., 2020). Many computers vision fields, such as image retrieval and video monitoring, use object detection.(Wu *et al.*, 2021).

#### 2.2.1.7 Object co-segmentation

As a special case of IS, object co-segmentation is the process of jointly segmenting objects that have semantic similarities across several images or video frames (Jerripothula *et al.,* 2017; Lu *et al.,* 2019; Zhang *et al.,* 2021; Zhang *et al.,* 2020).

## 2.3 Image Segmentation Techniques

There are different types of image segmentation techniques, each with its own advantages and limitations. Some of the most commonly used techniques are discussed in this section.

### 2.3.1 Cluster-based segmentation

Cluster-based segmentation is a technique used in image processing to segment an image based on the similarity of its pixels (Salvador and Chan, 2004). The process of clustering involves grouping the data points into a variety of groups so that the data points within each group are more similar to one another than to the data points within other groups. They are referred to as clusters (Dhanachandra *et al.,* 2015a).

Cluster-based segmentation has the benefit of allowing for the segmentation of images with complex colour or intensity distributions without the need for prior knowledge of the image's content. Cluster-based segmentation can, however, also be sensitive to noise and outliers in the data, and the choice of k can significantly affect how well the segmentation is done (Dubey and Vijay, 2018; Schroff *et al.,* 2015).

### 2.3.1.1 K-mean Clustering

By reducing the distance measure between the pixel and the cluster centroid, K-means clustering aims to divide an image into clusters that are mutually exclusive (Baldevbhai and Anand, 2012). With prior information about the image, the number of clusters is fixed (Chitade, 2010). Each pixel's distance from each cluster centroid, including the one where it is located, is determined. The pixels are redistributed to the closest centroid using this distance metric (Zeebaree *et al.,* 2017). As a result, a new centroid is determined using this pixel redistribution (Tiwari *et al.,* 2020). Once all of the pixels have been sorted to their closest centroid and the centroid values have stopped changing, the iterative step is finished. The K-means method is simple to program and computationally efficient (Dhanachandra *et al.,* 2015b). The outcome depends on the original cluster selection (Celebi and Kingravi, 2013). Table 2.1 shows the algorithm for K-means clustering.

**Table 2.1 K-means Clustering Algorithm**

Input: Image (I), with □ = {□1, □2, … , □□} pixels

□ = {□1, □2, … , □□} the quantity of clusters

1. Start
2. Place each pixel into any cluster at random.
3. Calculate the gap between each pixel and the centroid C= {□1, □, … , □□} as
   □ = ∑□−1 ∑□□‖□□ − □ ‖ ; □ ∈□ □ (2.1)
   Where ‖. ‖ denotes the Euclidean norm, □□ = mean of all pixels in kth cluster
4. Reassign the pixel □□ to the cluster □□ Iff ‖□□ − □ ‖2 ≤ ‖□ □ − □ ‖ ; 1 ≤ □ ≤ □
5. Once there has been no further reassignment, repeat the previous steps.
6. End.

### 2.3.1.2 Fuzzy C-mean Clustering (FCM)

An efficient and succinct segmentation algorithm is FCM clustering (Ganguly *et al.*, 2014). FCM is a data clustering approach in which a data set is divided into N clusters containing some data points in the dataset (Tolias and Panas, 1998). FCM clustering offers one data element that belongs to two or more clusters (Khang *et al.*, 2021). With the fuzzy c-Means algorithm, the data points can likely belong to more than one cluster, in contrast to the k-Means algorithm where they can only belong to one cluster. For overlapping data sets, fuzzy c-means clustering yields comparably better results (Bezdek, 2011).

**Table 2.2 Fuzzy C-mean Clustering**

Input: Image (I), with □ = {□1, □2, … , □□}
pixels C= {□1, □, … , □□} number of clusters
Output: Segmented image with C clusters

1. Start
2. Place each pixel into any cluster at random.
3. Calculate each pixel's level of cluster membership using

$$\square_{\square} = \frac{1}{\sum_{\square-1}^{\square} \frac{\square_{\square}}{\square_{\square\square}^{(2/\square-1)}}} \text{ where } \square_{\square} = \|\square_{\square} - \square\| \quad (2.2)$$

4. Reassign the pixel, *i* to the cluster, *j* with which it has large □□□ calculated using Equation (2.2)
5. Calculate the new cluster hub □□ as shown in equation 2.3:

$$\square_{\square} = \frac{\sum_{\square-1}^{\square}}{\sum_{\square-1}^{\square}} \quad (2.3)$$

6. Until convergence, repeat
7. End

Despite being a successful clustering method, FCM can be unreliable in noisy environments since the membership values it produces don't always accurately reflect

the degree of belonging of the data. FCM is additionally susceptible to image noise (Ghosh and Dubey, 2013).

### 2.3.2 Threshold-based segmentation

The allocation of pixel values in respect to the given threshold level is the focus of the IS technique known as thresholding. Each pixel's value is compared to the threshold value during thresholding (Bhargavi aand Jyothi, 2014). The pixel value is set to 0 if it is less than the threshold; alternatively, it is set to the maximum value (generally 255). Through the process of thresholding, we turn a colour or grayscale image into a binary image, or one that is only black and white (Khan *et al.,* 2022; Ratheash and Sathik, 2013).

#### 2.3.2.1 Colour Threshold-Based Segmentation (CT)

Based on the colour characteristics of the image pixels, CT segmentation assumes that homogeneous colours in the image correlate to distinct clusters and consequently, meaningful objects in the image. In other words, each cluster identifies a group of pixels with comparable colour characteristics.(Kulkarni, 2012).

#### 2.3.2.2 Adaptive Thresholding (AT)

A thresholding technique called AT accounts for fluctuations in illumination over space (SowparnikaB, 2014). The assumption of AT is that local areas of an image will have more consistent illumination and lighting than the entire image. In order to achieve superior thresholding outcomes, sub-regions of a picture are therefore examined and individually thresholded to produce the final output image (Bradley and Roth, 2007). A mean filter with the proper window size averages the divided image in AT into small sections. The segmentation of each sub-image is done using various threshold settings (Patil *et al.,* 2015). A binary image with the segmented sections is the output. Images

with varying illumination respond favourably to adaptive thresholding. The AT method's algorithm is shown in Table 2.3.

**Table 2.3 Algorithm for Adaptive Thresholding**

Input: Image (I), Window size (ws)

Output: binary picture in segments

1. Start
2. Normalize and subdivide I with mean or median filter using ws
3. Compute threshold $T_i$for each sub image, i$\epsilon$I
4. Each pixel is compared to.$T_i$
5. Depending on the threshold, assign to the forefront or the background
6. End

### 2.3.2.3 Global Thresholding (GT)

The GT approach, a single threshold value is used throughout the entire image (Padmasini *et al.,* 2018). The starting threshold $T_0$ for GT, an iterative procedure, is the average of all pixels. After grouping according to the chosen threshold $T_0$, a new threshold (T) is determined by averaging the mean pixel intensities for each group. Based on T, the pixels are reorganised. If there is a negligibly little difference between the new threshold and the prior one, this iterative procedure comes to an end (Abera *et al.,* 2017; Jang *et al.,* 2013). Table 2.4 presents the algorithm for the GT method.

**Table 2.48 Algorithm for Global Thresholding**

Input: Image (I)

Output: Binary picture in segments

1. Start
2. Set an initial threshold $T_0$ = mean ($\mu$) of all pixels
3. Divide the photos according to $T_0$
4. Recompute T as, T = ($\mu_1$ + $\mu_2$)/2
5. Iterate until T converge
6. End

### 2.3.3 Edge-based segmentation

In edge detection, segmentation is carried out end-to-end by locating the boundaries; edges are discovered in order to locate image discontinuities. The edges that are recognised in edge-based detection don't have to be closed. During segmentation, finding edges or pixels enables us to extract or connect pixels to create closed object boundaries (Mueller *et al.*, 2004). Edge Detection is the act of finding and locating sharp with fine discontinuities, and this method aids in obtaining the desired results (Bräunl *et al.*, 2001; Gao *et al.*, 2010). Using edges as a criterion, objects are identified using this method. The first order derivative/gradient operator, the second derivative operator, and the optimal edge detector are commonly used to identify these items (Canny, 1986; Vincent and Folorunso, 2009).

#### 2.3.3.1 Gradient operator

Any time the intensity level is discontinuous, the gradient operator, which uses first order derivatives, reacts. Prewitt, Roberts, and Sobel operators, which identify edges by determining the magnitude in their first derivative, have a positive leading edge and a negative following edge (Saif *et al.*, 2016).

#### 2.3.3.2 Second derivative operator

When the lighter side is negative and the darker side is positive, use the second derivative operator. It is extremely susceptible to picture noise. However, it is particularly helpful for obtaining some secondary data, such as the Laplacian operator and Difference of Gaussian (DoG), which detect edges by looking for zero-crossing. (Karanwal, 2021; Srinivasulu and Premkumar, 2021).

#### 2.3.3.3 Optimal edge detector

The most effective edge detector can create noise-resistant, continuous edges that are only one pixel thick. It can also recognise sharp and jagged edges (Bharodiya and Gonsai, 2019; Pithadiya *et al.*, 2009). There are various reasons why the edge-based segment is poor. The first reason is that the technique fails to produce the object boundaries. The rationale is because it enables missing and irregular boundaries to be used to delineate the region of interest (Rao and Ben-Arie, 1994).

The edge-based segmentation method can be implemented as follows:

i. Load the image: Load the grayscale image or load rgb image and convert to grayscale image. Convert the image to double precision to perform the required computations.
ii. Compute the edge map: Compute the gradient magnitude of the image using the Sobel operator or any other edge detection algorithm. The edge map is a binary image that highlights the edges in the original image (Mushtaq *et al.*, 2022).
iii. Initialize the contour: Choose an initial contour that defines the object boundary. This contour can be a simple geometric shape such as a circle, rectangle or polygon. You can also use a previously segmented object as the initial contour (Iannizzotto and Vita, 2000; Priyadharsini and Sharmila, 2019).
iv. Evolve the contour: Use an iterative process to deform the initial contour towards the object boundary. The evolution process should be guided by the edge map such that the contour stops at the edges of the object.
v. Stop the evolution: Stop the evolution process when the contour converges to the object boundary. This can be achieved by setting a convergence criterion based on the change in contour position between iterations.

vi. Refine the contour: Refine the final contour by smoothing it and removing any jagged edges.

vii. Extract the segmented object: Use the final contour to extract the segmented object from the original image (Haoran *et al.*, 2019).

### 2.3.4 Region-based segmentation

A region of an image, indicated by the letter R, is defined as a linked, homogenous subset of the image in terms of some criterion, such as texture or grey level. A region in a picture is a collection of related pixels having the same characteristics (Soomro *et al.*, 2018a; Xiaohan *et al.*, 1992). The region technique assigns each pixel to a specific object or region. In the region-based segmentation technique, nearby pixels are compared for similarity. In other words, pixels with comparable characteristics are categorised into separate zones. The image is divided into portions by region-based segmentation algorithms that look for related features (Singh and Kaur, 2019). The method finds these regions, which are merely groups of pixels, by first selecting a seed point, which could be a little or substantial chunk of the input image. Region-based segmentation algorithms are more controllable and noise-resistant than edge detection methods (Arulmurugan and Anandakumar, 2018; Su *et al.*, 2018). While region-based approaches divide an image into close parts in accordance with a set of specified criteria, edge-based methods divide an image based on sharp reforms in intensity near edges (Nair, 2018; Wazarkar *et al.*, 2018).

The region-based segmentation collects and labels the pixels that relate to an item. The employment of suitable thresholding methods is also necessary for region-based segmentation. The crucial concepts are spatial closeness and utility similarity (both have grey value variance and differences) (which consists of Euclidean distance and

compactness of a region) (Mueller *et al.,* 2004; Tian *et al.,* 2009). Following are the main techniques used in region-based segmentation algorithms:

#### 2.3.4.1 Region growing

Region Growing refers to the capability of deleting a linked region of the image based on certain predetermined criteria. Based on information about intensity, this criterion. An approach to picture segmentation known as "region expanding" looks at nearby pixels and joins them to a region class where no borders are found (Zhou *et al.,* 2018). This technique is repeated numerous times for each boundary pixel in the area. If neighbouring regions are discovered, a region-merging technique that eliminates weak edges while maintaining strong edges is applied (Li *et al.,* 2018; Raja *et al.,* 2018). Table 2.5 presents the algorithm for region growing.

**Table 2.5 Region Growing Algorithm**

Input: Image (I)

Output: Segmented image

1. Start.
2. First, choose some seed pixels for the picture.
3. Then, a region develops from each seed pixel:
4. Set the region prototype to be the seed pixel after that.
5. Determine how closely the candidate pixel and the region prototype resemble each other.
6. Additionally, determine how similar the candidate is to its nearby neighbour.
7. If both similarity measures are greater than the experiment's predetermined thresholds, the candidate pixel is included.
8. Then compute the new principal component to update the region prototype.
9. Finally, go to the subsequent pixel to be studied.
10. End

When compared to other colour IS techniques, this algorithm offers a number of benefits. The expanding technique is straight forward. Growing regions are discovered to have precisely thin and continuous borders. In terms of noise, the algorithm is likewise highly steady. The only drawback is that it needs a seed point, which usually entails manual intervention. In order to segment each region, a seed point is required.

#### 2.3.4.2 Region splitting and merging

The split-and-merge strategy is the antithesis of regional expansion. This method utilises the entire image. Top-down strategies involve region division. It starts with a full image and slices it so that the segregated slices are more homogenous than the whole image (Peng *et al.*, 2020). Single segmentation is inadequate for logical segmentation since it severely restricts segment shape. Therefore, the split-and-merge algorithm splitting followed by a merging phase is always preferred (Zhang *et al.*, 2020). Any region can be divided into smaller regions, and the suitable regions can be combined to form a larger region. In an effort to serve the shapes of rational IS, the user can split a picture into a number of random, unconnected areas rather than selecting kernel points, and then merge the regions. The theory based on quad tree data is typically used to split and merge regions. An image-segmentation method that takes geographical information into account is region splitting and merging (Basar *et al.*, 2020; Dorninger and Pfeifer, 2008). Table 2.6 shows the region-splitting and merging algorithm.

**Table 2.6 Region-splitting and merging algorithm**

Input: Image (I)

Output: Segmented image

1. Start
2. Start by looking at the entire picture.
3. Divide the variation into quadrants if it is too large.
4. Any adjacent regions that are similar enough should be merged.
5. Continue performing steps (b) and (c) until there is no longer any splitting or merging.
6. End

### 2.3.5 Energy-Based Segmentation

Energy-based segmentation is a method of image segmentation that is based on minimizing an energy functional (Bartesaghi *et al.,* 2005). The energy functional is a mathematical representation of the image and is defined in terms of various energy terms that represent different aspects of the image, such as brightness, contrast, texture, and boundaries. The goal of energy-based segmentation is to find the optimal segmentation of the image that minimizes the energy functional (Sebastian *et al.,* 2020). The segmentation findings are reflected in the minimal solution .

The process of energy-based segmentation involves the following steps:

i. Formulate the energy functional: The first step in energy-based segmentation is to formulate the energy functional that represents the image. This involves defining the energy terms that represent different aspects of the image.

ii. Minimize the energy functional: The next step is to minimize the energy functional to obtain the optimal segmentation of the image. This is typically done using numerical optimization techniques such as gradient descent or convex optimization (Birchfield *et al.,* 2007).

iii. Evaluate the segmentation: Once the optimal segmentation has been obtained, it is evaluated to determine its quality. This can be done using various metrics such as precision, recall, F1 score, and intersection-over-union (IoU).

iv. Refine the segmentation: If the segmentation is not satisfactory, it can be refined by adjusting the energy terms or the optimization parameters and repeating the optimization process.

Energy-based segmentation has been used in various applications such as object recognition, medical image analysis, and remote sensing. It offers a powerful framework for image segmentation that can incorporate various aspects of the image in a unified manner. However, it requires careful tuning of the energy terms and optimization parameters, and can be computationally intensive (Hagenmuller *et al.*, 2013; Li *et al.*, 2018).

The most popular techniques in this area are active contour and graph-based techniques (Sebastian *et al.*, 2020).

#### 2.3.5.1 Active contour

It has been extensively employed in a range of applications during the past ten years, including picture segmentation and motion tracking. Active contour basically seeks to modify a starting curve to the boundary of an object under specified restrictions from the image (Liu *et al.*, 2020). The two fundamental models in active contour that are addressed in terms of implementation are snakes and level sets. According to an energy-saving method, snakes relocate to designated snake sites. In level set, the contour is moved expressly in accordance with a specific level of function. Active contour models are frequently employed because they have numerous appealing advantages over conventional picture segmentation techniques, such as region growth, thresholding, and

edge detection. First of all, active contour models allow for the consolidation of various prior knowledge and can be figured efficiently within a framework of principled energy minimization. Second, they may produce segmentation outputs with closed and smooth contours, which are fundamental and can be employed right away in other applications, such shape analysis and recognition (Teng *et al.,* 2019). Additionally, the active contour method—a quick and effective way to locate object boundaries—was widely employed for picture segmentation. There are two types of edge-based and region-based active contours. An edge detector is frequently used for edge-based to define the boundaries of picture regions and draw contours to these limits. Edge-based active contours may ignore the hazy borders in images because the picture gradient technique is used in both edge-based segmentation and EAC. For the image I(x, y), the edge functional is given in equation 2.1.

$$E\_edge = -|\nabla I(x,y)|^2 \quad (2.1)$$

To develop the contour for region-based, statistical data on the picture intensities are used (M. Zhang *et al.,* 2020). Due to global energy minimization, region-based active contours frequently have no limits on where to position the initial contours. For better understanding the region-based formula is as follows: Find the Contour C, which divides the picture into non-overlapping parts, given image *I*. Equation 2.2 gives the model energy function.

$$□(□_1, □_2, □) = □ \int_{□□□□□□(□)} |□(□) - □_1|^2 \, □□ + □ \int_{□□□□□□□(□)} |□(□) - □_2|^2 \, □□ + □|□| \quad (2.2)$$

Where □ is a constant, and C is any other variable curve, and *inside(C)* and *outside(C)* denote the regions inside and outside the contour C, correspondingly, and the constants $□_1$, $□_2$ dependent on C, is the average image intensity in inside C and correspondingly outside C.

The region-based active contour may identify internal borders regardless of where the initial contours are located. The application of pre-defined start contours provides a way of autonomous segmentation. Additionally, compared to active contours based on edges, they are less vulnerable to local minima or noise. Thus, the fundamental segmentation issue of initialising active contour is one (Mondal, 2019).

#### 2.3.5.2 Graph methods

It depends on methods based on graph theory. This group of segmentation techniques works by finding the smallest cuts in a graph, with the cut criterion trying to reduce the similarity between the separated pixels (Basavaprasad and Hegadi, 2014; Lu *et al.*, 2019; Peng *et al.,* 2013). Graph techniques come in a variety of forms, including Normalize cut, Graph-cut, and Local Variation.

i. Normalise cut**:** A graph approach called normalise cut views an image pixel as the anode of the graph and views division as a chart apportioning problem. It is shown that the picture is an undirected, weighted diagram (Dimauro and Simone, 2020; Ibrahim and El-Kenawy, 2020). Every pixel is a node in the graph, as well as every pair of pixels is an edge. The comparability of the pixels is gauged by the weight of an edge. By eliminating the boundaries that connect the parts, the image is split into separate sets. The distribution of the graph that minimises the weights of the removed edges is considered optimal *(*Eriksson *et al.*, 2010; Shi and Malik, 2000).

ii. Graph–cut: A optimal solution for binary labelling as foreground and background picture segmentation can only be found via graph-cut. Where the object meets the background is where the cut should be made. In particular,

energy should be reduced close to the object boundary (Freedman and Zhang, 2005; Yi and Moon, 2012).

iii. Local variation**:** It resembles normalised cuts in certain ways. The weights at each edge calculate the disparity between pixels. Based on the degree of variability in nearby regions, this technique separates an image into segments (Baek *et al.*, 2022; Wang *et al.,* 2011). Dealing with the issue of under or over segmentation is another issue in IS that has been addressed. Methods based on graphs have drawbacks. is highly computational to start. It also responds to over and under segmentation. Thirdly, there is a necessity for user interaction and time complexity (Xu *et al.*, 2021).

The general implementation of graph-based segmentation involves the following steps (Camilus and Govindan, 2012; Mushtaq *et al.*, 2022):

i. Constructing the graph: The first step is to construct a graph from the image. This can be done by representing the pixels of the image as nodes in the graph and connecting each node to its neighboring nodes.
ii. Computing edge weights: The next step is to compute the edge weights between the nodes. This can be done using different techniques such as the intensity difference between neighboring pixels or the colour difference between neighboring pixels.
iii. Partitioning the graph: After computing the edge weights, the graph is partitioned into regions using graph partitioning algorithms such as spectral clustering or minimum-cut algorithms. These algorithms use the edge weights to group the nodes of the graph into different regions (Strîmbu and Strîmbu, 2015).

iv. Post-processing: The final step is to perform post-processing on the segmented regions. This can involve merging small regions, removing noise or smoothing the boundaries between the regions (Strom *et al.*, 2010).

### 2.3.6 Watershed segmentation

Watershed segmentation is a popular technique used for image segmentation that is based on the principles of mathematical morphology. With this method, an image is treated like a topographical map, with the brightness values representing the height of the terrain and the borders between sections representing peaks and valleys (Amin *et al.*, 2017).

Watershed segmentation works by flooding the image with water from the catchment basins or watersheds, letting it collect in the valleys or low-lying areas, and then letting it overflow into the adjacent catchment basins. The segmentation regions or labels are then created using the catchment basins (Babu *et al.*, 2017).

The general steps for watershed segmentation are as follows:

i. Create a gradient image using the source image. This can be achieved by highlighting the edges and boundaries between various sections in the image using various gradient operators, such as the Sobel, Prewitt, or Laplacian operators (González-Betancourt *et al.*, 2017).

ii. Decide which seeds or markers will be utilised to initiate the flooding operation. These markers, which should be put on the image's regions of interest, can be manually chosen or created automatically using methods like thresholding, edge detection, or clustering.

iii. Use the markers as starting points for calculating the gradient image's distance transform. This transform directs the flooding process by assigning a distance value to each pixel in the image based on its separation from the closest marker.

iv. Apply a flooding algorithm on the distance transform picture, such as the watershed transform or the morphological watershed algorithm. The catchment basins are gradually filled with water from the markers using this method, which then allows the water to overflow into the adjacent catchment basins to imitate the flooding process.

v. The resulting segmentation image should then be post-processed to get rid of any undesirable regions or noise and to make sure that the regions are connected and labelled correctly.

#### 2.3.6.1 Over-segmentation watershed

This type of transformation involves first turning the image into a gradient image, which is then given the watershed transform. As a result, the image is excessively segmented into a large number of small sections, each of which corresponds to a local minimum or catchment basin in the gradient image (Jia *et al.,* 2020; Ng *et al.,* 2006). This method can be used to find all local minima or objects in an image, and it can be combined with another method for merging the regions into larger objects.

#### 2.3.6.2 Under-segmentation watershed

In this case, an initial segmentation approach, such as thresholding or clustering, is used to first divide the image into a few sizable parts. To further define the borders between the sections, the gradient image of the segmented regions is then transformed using the watershed method. This method can be applied to enhance the smoothness or accuracy of an initial segmentation, and it can be followed by post-processing to eliminate any undesired regions or artefacts (Kenneth *et al.,* 2019; Ng *et al.,* 2006).

The usage of any method of watershed segmentation relies on the particular application and image properties, as both offer benefits and drawbacks. For instance, over-

segmentation watershed can be used to detect small objects or regions of varied intensities, whereas under-segmentation watershed can be used to improve an initial segmentation or smooth out noisy boundaries.

## 2.4 Related Works

Comparative analysis of six key segmentation techniques: clustering, edge-based, fuzzy logic, neural network, region-based and thresholding was presented by Max Jayapriya and Hemalatha (2019). The clustering technique was shown to have a long computing time in this investigation, whereas the edge-based was not suited for low contrast images. The fuzzy logic technique's shortcoming was the difficulty in determining fuzzy membership. When segmenting overlapped grayscale pixel values, the region-based method was found to be challenging, while the thresholding technique was shown to be computationally expensive. This study recommended marker-based controlled watershed segmentation as a suitable method for medical IS because it has minimal over-segmentation problems. However, this recommended marker-based controlled watershed segmentation technique suffers from an under-segmentation problem (Kenneth *et al.*, 2019).

Adegun *et al*. (2018) gave a thorough overview of the most recent algorithms and methods for segmenting and classifying large-scale satellite imagery with the primary goal of identifying land use. The examination of remote sensor images and a review of the effectiveness assessments of a few recently created algorithms are used to compare the various methods currently in use for classifying land use. It was found that the application of machine learning techniques like deep learning for performing land use classification through pattern analysis of satellite imagery is encouraged by technological advancements and the availability of a large and voluminous data set for training the machine learning algorithms. The study revealed that most of the state-of-

the-arts deep learning methods performed reasonably well with average accuracy result of 75%. The drawback of this study is that the limitations of the state-of-the-art methods were not discussed, and the performance of the state-of-the-art methods were evaluated using only accuracy or f-score.

Driven by the requirement to enhance macroeconomic forecasts and reduce their time horizons, Juergens and Meyer-Heß (2021) concentrated on utilising very-high-resolution (VHR) photographs to identify construction regions and their temporal variations to approximate construction spending as a driving force for economic forecasting. To discover construction zones and their temporal advancement, WorldView pictures from a location around the southern portion of Berlin, Germany, were subjected to multi-resolution segmentation accompanied by a K-Nearest Neighbor (KNN) categorization. Construction zones have different material compositions than other land cover groups, resulting in distinct classification patterns. From the VHR picture, several sorts of sealed zones, like commercial or residential, may be distinguished. The identification of water, which is frequently classed as a sealed surface, is a significant problem for this paper. This is because there are only a few water samples in the scenarios.

U-Net with ResNet encoder was adapted by Liu *et al.* (2020) for performing remote image segmentation for building extraction. The first step was the collection of remote sensing images through some open datasets, and then the building images were outlined to get the building masks. A training data set and a validation set were created from the dataset. The training dataset which 80% of the initial dataset was used to train the U-Net model. The model reached a Mean Intersection over Union (MioU) of 0.83. The proposed U-Net with ResNet encoder can effectively segment buildings with clear

boundaries. Nonetheless it performs poorly when presented with buildings with too smooth and curved boundaries.

By combining satellite imagery with multiresolution, multisensory, and multitemporal data, Rudner *et al*. (2019) proposes a revolutionary method for quickly segmenting flooded buildings (CNN). The CNN network is made up of numerous streams of encoder-decoder architectures that combine spatial and spatiotemporal information from high-resolution photos and medium-resolution images to create a single segmentation map of flooded buildings at a medium resolution. A map is produced by the encoder-decoder streams using information from a single sensor. If there is information from numerous sensors, the streams are combined to create a joint prediction map. Through the use of many satellite sensors, the approach attempts to speed up the process of creating flood maps based on satellite data. At least one successful satellite image acquisition can be used to create segmentation maps, which can then be enhanced when more imagery becomes available. The model's high computational complexity is a significant drawback.

Kushwah and Markam (2021) performed satellite image segmentation of satellite images using deep learning. In the study the satellite images were cropped into patches and provided with labels. The U-net model was trained on each label one after the other, then the multiple outputs were combined to segment the images. The images were segmented into 10 classes. The model achieved a precision and recall of 93.11% and 73%, respectively. The proposed model suffers from high requirement of computational power and time.

The paper by Sharifzadeh *et al.* (2020) concentrated on detecting farms using low quality satellite photos. The entire framework comprises of semantic segmentation of detected farm patches in order to locate farm pixels, followed by local patch or Region

of Interest (ROI) categorization. In the first step of the framework, two main patch classification methodologies were used; first, a conventional hand-crafted feature extraction and modelling strategy was constructed. The detection of green areas in this method was accomplished through unsupervised thresholding utilising the Normalized Difference Moisture Index (NDMI). Then, to distinguish the farm patches from other patches that do not contain any farms, a two-step approach was created using the Grey Level Co-occurrence Matrix (GLCM), 2D Discrete Cosine Transform (DCT), and morphological features. The second patch classification method is based on in-depth, high-level features that were learned from the networks of the Visual Geometry Group (VGG-16) before to training. Transfer learning techniques were used to classify farms based on these parameters. After that, farm pixels were semantically separated from local patches in the second step of the framework. The networks were retrained using four different pretrained networks resnet18, resnet50, resnet101, and mobileNet along with tagged patches. Experimental findings demonstrated that CNN models are superior in terms of patch categorization accuracy for the first stage of the framework (99.55 percent and 96.76 percent for train and test respectively). The resnet50 reached the best overall accuracy for semantic segmentation for the second phase of the framework (90.38% and 82.84% for train and test respectively). The model's significant computational complexity is a flaw.

A comprehensive evaluation of image segmentation strategies was presented by Abdulateef and Salman (2021). In this study, four segmentation strategies are discussed: threshold-based, edge-based, region-based, and energy-based segmentation. Each technique's benefits and drawbacks were discussed. It was found that not all technologies are appropriate for all types of photographs and that not all procedures are best for all types of images. However, no experimentation results were published in this

work to illustrate how well any of the presented methods performed on image segmentation.

In order to quickly segregate flooded pixels in freely available Copernicus Sentinel-1 Synthetic Aperture Radar (SAR) data, Nemni *et al*. (2020) developed a CNN-based approach that requires no optical bands and little pre-processing. The U-Net, XNet and a combination of U-Net and ResNet CNN models were both utilized in the study. The method got an accuracy of 99%. Precision of 82%, recall of 97%, critical success index of 0.79 and Dice of 0.89. However, the model is computational expensive.

Hemalatha *et al.* (2018) used active contour segmentation algorithms to analyse medical images. For the target object's portions intended for segmentation, the active contour establishes a distinct boundary or curvature. The classification of the contour into several types, such as gradient vector flow, balloon, and geometric models, depends on a variety of criteria. The problem with the segmentation approaches currently in use is that the search process cannot contract and expand until it is known where to begin.

Ulmas and Liiv (2020) employed a CNN with an altered U-Net architecture to construct land cover categorization maps derived from satellite data. The study's purpose was to train and evaluate CNN models for autonomous land cover mapping, as well as to see how effective they were in improving accuracy and detecting changes. The Big Earth Net satellite picture collection was used in this investigation. The built classification model had a high average F1 score of 0.749 on multiclass land cover classification with 43 probable picture labels. In the Big Earth Net dataset, the algorithm also identifies noisy data, such as photos with inaccurate classifications. The model showed a high Mean Intersection Over Union (MioU) score ranging from 0.76 to 0.87 for land cover classes like woods, inland lakes, and arable land. The suggested model is not ideal for

machine learning-based segmentation, as it has higher accuracy in some classes but lower results in visually less different classes.

Sadiq *et al*. (2019) suggested a combination of histogram, active contour, and edge detection for segmentation of satellite images. To test the model the Landsat 7 imagery was used. The histogram method was first used to detect the range of each peak in input images, then this detected range is used as the threshold to generate the mask in the active contour algorithm. Finally, the edge detection algorithm is then implemented to detect the edges and generate the final template of each interesting region. The generated edge template was then applied on the original input image to separate the different regions on input image. However, the suggested model cannot separate weak boundary, fuzzy boundary, or discontinuous boundary object.

The study by Park and Lee (2019) performed forest disaster detection using satellite images with semantic segmentation. The satellite image dataset used was collected from Landsat satellite and the images were applied to the detection of impaired area using U-Net Ronneberger *et al.,* (2015) and SegNet models. U-Net and SegNet was trained using 2,200 training data with varying optimizers, epochs, and learning rates, and tested with 3 images after training process. U-Net achieved an accuracy of 97.9% and SegNet obtained an accuracy of 96.9%. Since training may slow down in the middle layers of deeper models due to the limitations of the methods now in use, there is a chance that the network learning may overlook the levels where abstract features are represented.

Ye *et al.* (2018) proposed a new remotely sensed edge detection technique that uses fast Guided filters to improve the image quality, then an upgraded Sobel operator with a 3 by 3 mask and eight directional templates to discover gradients and gradient orientations. A new two-dimensional Ostu approach was used to choose high and low thresholds. The PNG photographs of the University of the Chinese Academy of

Sciences were utilised in the experiment. Although the suggested approach provides more edge details, crisp and continuous outlines, it has two drawbacks: high time complexity and inefficiency when dealing with high-intensity noise.

Popescu *et al.* (2018) developed a new technique for detecting locations of interest, such as floods in rural areas, utilising photos from unmanned aerial vehicles (UAVs) and graphics processing units (GPU). The supervised masks of flood segmentation in the pictures from the learning set is created using the conventional GPU through parallel computation of textural features taken from the co-occurrence matrix. The weights of the generator and discriminator are established using these images and the real masks that go along with them. For the learning phase, 40 images were used, and for the technique validation, 60 images were used. The method achieved an accuracy between 89-95.5%. The drawback of the GAN method is relatively hard to train and takes a long time to learn.Table 2.1 gives a summary of the related literature.

**Table 2. 7 Summary of Related Works**

| S/N | AUTHOR(S) | TECHNIQUE | STRENGTH | WEAKNESS |
|---|---|---|---|---|
| 1 | Jayapriya and Hemalatha (2019) | Clustering, edge-based, fuzzy logic, neural network, region-based and thresholding | Provides comparative analysis of six key techniques. Additionally suggested as a good method for medical IS due to its low over-segmentation issues is marker-based controlled watershed segmentation. | The recommended marker-based controlled watershed segmentation technique suffers from an under-segmentation problem |
| 2 | Adegun *et al.* (2018) | Deep learning | Detailed survey of the state-of-the-art algorithms and techniques for performing image segmentation and classification of large-scale satellite imagery | The study's flaw is that the constraints of the cutting-edge techniques were not explained, and their performance was assessed solely by their accuracy or f-score. |
| 3 | Juergens and Meyer-Heß (2021) | K-Nearest Neighbor (KNN) | Capable of identifying construction regions and their temporal variations | The identification of water, which is frequently classed as a sealed surface, is a significant problem for this paper. This is because there are only a few water samples in the scenarios. |
| 4 | Liu *et al*. (2020) | U-Net with ResNet Encoder | Trainable with a small dataset | Performs poorly when presented with buildings with too smooth and curved boundaries. |

| S/N | AUTHOR(S) | TECHNIQUE | STRENGTH | WEAKNESS |
|---|---|---|---|---|
| 5 | Rudner *et al.* (2019) | Convolutional Neural Network (CNN) | aims to speed up the process of creating flood maps using satellite photography by combining data from various satellite sensors. | Computationally complex |
| 6 | Kushwah and Markam (2021) | U-net | Robust segmentation with ten segment classes | Suffers from high requirement of computational power and time. |
| 7 | Sharifzadeh *et al*. (2020) | Support Vector Machine (SVM), VGG-16, resnet18, resnet50, resnet101and mobileNet | Automatically detects the important features | Computationally complex |
| 8 | Abdulateef and Salman (2021) | Threshold-based, edge-based, region-based, and energy-based segmentation | Provides comprehensive evaluation | No experimentation results were published in this work to illustrate how well any of the presented methods performed on image segmentation. |
| 9 | Nemni *et al.* (2020) | CNN | High performance of up to 99% accuracy | Computational expensive. |
| 10 | Hemalatha *et al*. (2018) | Active contour | It's easy to follow an object on subsequent similar images. | The issue with the proposed techniques is that it must know where to start the search process before it can contract and expand. |

| S/N | AUTHOR(S) | TECHNIQUE | STRENGTH | WEAKNESS |
|---|---|---|---|---|
| 11 | Ulmas and Liiv (2020) | CNN | Identifies noisy data and diversified class labels | The suggested model is not ideal for machine learning-based segmentation, as it has higher accuracy in some classes but lower results in visually less different classes. |
| 12 | Sadiq *et al.* (2019) | Histogram, Active contour, and Edge detection | Suitable for sharp intensity boundaries | Cannot separate weak boundary, fuzzy boundary, or discontinuous boundary object. |
| 13 | Park and Lee (2019) | U-Net and SegNet | Learns deep features that produces high performance | There is some risk that the network learning will disregard the layers where abstract characteristics are represented since learning may slow down in the middle layers of deeper models. |
| 14 | Ye *et al*. (2018) | Sobel and fast Guided filters | Ability to provides more edge details, crisp and continuous outlines | High time complexity and inefficiency when dealing with high-intensity noise. |
| 15 | Popescu *et al.* (2018) | Generative Adversarial Networks (GAN) | Achieve relatively high performance | hard to train |

# CHAPTER THREE

## 3.0 RESEARCH METHODOLOGY

The procedures utilised to conduct this research are described in this chapter. Data gathering, image processing, feature extraction, and data classification are some of these methods. Figure 3.1 provides an illustration of the suggested system.

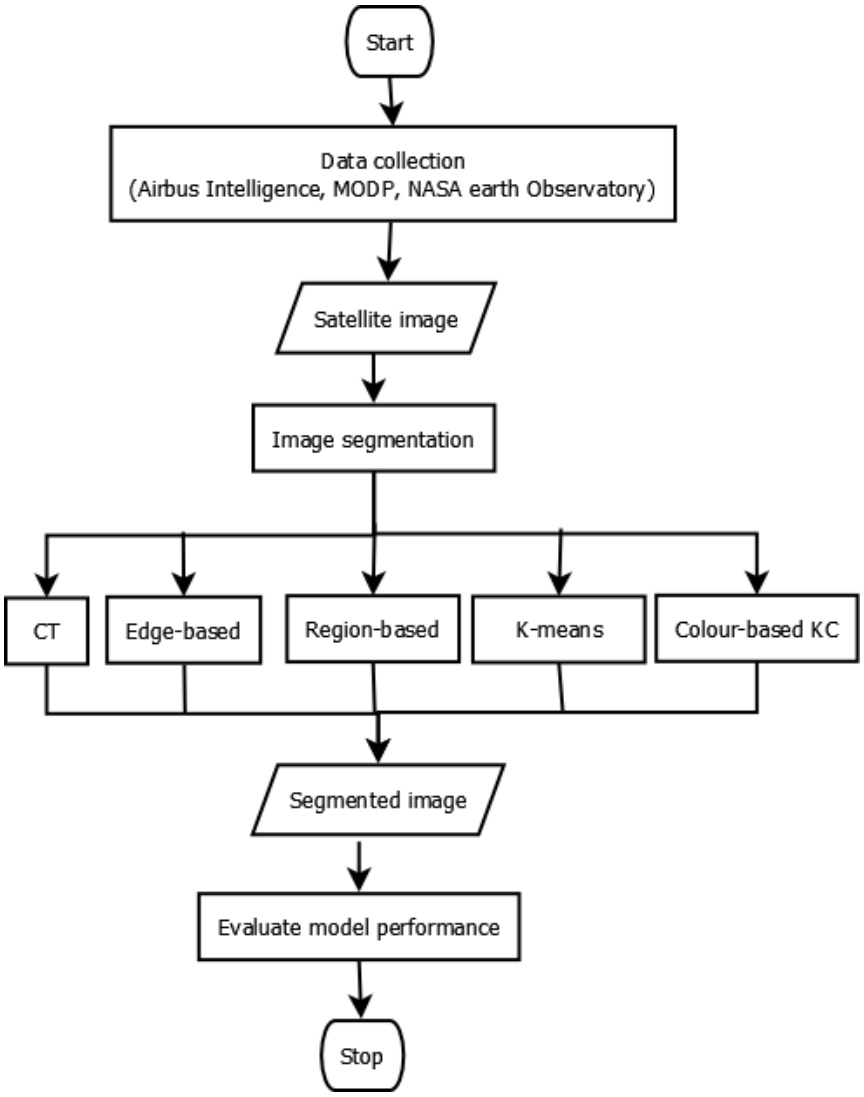


Figure 3.1 Block Diagram of the Research methodology

### 3.1 Dataset

A dataset is refered to as a collection of examples used for training or testing machine learning models. Airbus Intelligence (Airbus Intelligence, 2021), NASA Earth

Observatory (NASA, 2021) and Maxar Open Data Program (MODP) (Maxar, 2021) were used to acquire data for this investigation. MODP is a rescue-in-action satellite imagery catalogue that is free and available to the public. The MODP was created to aid rescue missions in disaster management and emergency response. MODP gives brief descriptions and photographs of natural disasters such as hurricanes, tornados, wildfires, floods, explosions, and earthquakes. NASA's Earth Observatory houses satellite photos, stories, and findings of the environment, earth systems, and climate resulting from NASA research. Airbus Intelligence is a satellite imagery gathering, data processing, fusion, distribution, and intelligence collection expert. High-resolution SPOT satellite imagery is also included in the Airbus Intelligence. Figure 3.2 is an example of the Airbus Intelligence satellite imagery used in this study.

Figure 3.2 Sample of Airbus Intelligence satellite imagery

The data collected was analysed using a hybridization of both colour threshold-based and K-means clustering image segmentation techniques. This involved first preprocessing the data using decorrelation stretching and histogram equalization techniques to improve the image quality and enhance the features in the images.

The colour threshold-based segmentation was then applied to the preprocessed images to detect regions of interest with a specific colour range. The K-means clustering segmentation was then applied to the same preprocessed images to group similar pixels into clusters. These two segmentation techniques were then combined to produce a more accurate flood detection in satellite imagery. To evaluate the performance of the hybridized segmentation technique, precision, recall, Intersection-over-Union (IoU), F1 score, and Dice similarity coefficient (DSC) metrics were used. These metrics were used to assess the accuracy of the flood detection by comparing the results obtained from the hybridized segmentation technique to the ground truth data. The ground truth data was manually annotated by experts to identify the areas that were affected by the flood. The evaluation showed that the hybridized segmentation technique achieved high accuracy in detecting flooded areas in satellite imagery.

## 3.2 Image Enhancement

Image enhancement is the technique of enhancing an image's visual appeal or making it more analytically or interpretively valuable. The primary goal of image enhancement is to improve the image's quality for usage in computer vision applications or for human perception. Digital images are modified during the process of image enhancement to provide outcomes that are better suited for display or additional image analysis. To make it simpler to spot important details, you can, for instance, eliminate noise, sharpen, or brighten an image. Image enhancement techniques can be applied to a variety of images, including photographs, satellite imagery, medical images, and surveillance footage. The choice of technique depends on the specific application and the characteristics of the image being enhanced.

There are several methods for image enhancement, including:

i. Histogram equalisation: This process stretches the distribution of pixel intensities to increase contrast in photos.

ii. Sharpening: A method for sharpening edges and details in an image by boosting contrast along the edges.

iii. Filtering: A method for eradicating noise from images or blending them to soften transitions.

iv. Colour adjustment: A method for enhancing certain colours or changing the colour balance of an image to remove colour casts.

v. Tone mapping: A method for reducing an image's dynamic range so that it will display more effectively on devices with constrained dynamic range.

Histogram equalisation and decorrelation stretching were utilised in this work as two image enhancing techniques.

### 3.2.1 Histogram equalisation

After collecting the RGB satellite imagery, the images were preprocessed using the Histogram Equalisation image enhancement technique. Image enhancement was performed at this stage because it highlight the more refined features in the coloured satellite imagery and highlight the important information .

Compared to grey images, colour images contain more and richer information for visual perception. In Digital Picture Processing, colour image enhancement is critical. The pictures appear darker or with little contrast when the lighting is poor. Images with low contrast must be improved. The histogram equalisation approach is applied in this investigation. Histogram Equalisation is a technique for adjusting contrast in images by using the histogram . The goal of this technique is to remap the scene's histogram to a

distribution with a probability density function that is almost uniform.The equalisation of the histogram redistributes the intensity distribution. If an image's histogram has a lot of peaks and valleys, it will still have peaks and valleys after equalisation, but they will be moved. Histogram Equalisation is a technique for improving contrast and obtaining a homogeneous histogram.

The step by step implementation of the Histogram Equalization is as follows:

i. Start.

ii. Load the input image.

iii. Convert the input image to grayscale if it is in colour.

iv. Compute the histogram of the input image.

v. Compute the cumulative distribution function (CDF) of the histogram.

vi. Normalize the CDF.

vii. Compute the new intensity values for each pixel using the normalized CDF.

viii. Create a new output image with the same dimensions as the input image.

ix. Set the intensity value of each pixel in the output image based on the new intensity values computed in step 6.

x. Save the output image.

xi. End.

### 3.2.2 Decorrelation stretching

When there is strong band-to-band correlation in an image, de-correlation stretching improves the colour differentiation. Exaggerated colour contrast enhances visual comprehension and facilitates feature recognition. The decorrstretch function in matlab

was used for the decorrelation stretching. Typically, there are three colour bands, or NBANDS, in an image. Nevertheless, de-correlation stretching can be used despite the quantity of colour bands. The image's original colour values are translated into a new set with a larger variety of colours. Each pixel's colour intensities are stretched to equalise band variances before being turned back into its original colour bands. This process involves transforming each pixel's colour intensities into the colour eigenspace of the NBANDS-by-NBANDS covariance or correlation matrix.

The basic steps for Decorrelation Stretching are presented below:

i. Start.
ii. Load the input image.
iii. Convert the image to grayscale if it is in colour.
iv. Compute the covariance matrix of the image.
v. Compute the eigenvalues and eigenvectors of the covariance matrix.
vi. Sort the eigenvalues in descending order.
vii. Choose the top K eigenvalues and their corresponding eigenvectors.
viii. Compute the transformation matrix using the chosen eigenvectors.
ix. Apply the transformation matrix to the original image to obtain the decorrelated image.
x. Normalize the decorrelated image to a desired range of values.
xi. Save the output image.

xii. End.

## 3.3 Image Segmentation

The next step after performing the image enhancements is the image segmentation. Given that the important information and more refined features have been highlighted by the image enhancements technique, it is then appropriate to perform segmentation on the images. The enhanced images were segmented using four renowned techniques: Edge-based Active Contour (EAC), Region-based Active Contour (RAC), Colour Thresholding (CT) and Colour-based K-means Clustering (Colour-based KC). To have a better understanding of image segmentation figure 3.3 shows an input satellite image before segmentation and figure 3.4 depict an output image with the segmented flooded area.

Figure 3.3 Sample of Input Image

Figure 3.4 Image after segmentation

Image segmentation is typically a technique of disintegrating a digital photo into subgroups.

Image segmentation is a method of breaking down a digital image into smaller groupings termed "image segments" to reduce the complexity of the image and make future editing and evaluation easier.

### 3.3.1 Edge-based active contour (EAC)

Edge-based segmentation looks for inconsistencies in an image's intensity. A border between two locations with significantly distinct attributes can be characterised as an edge. EAC is based on the idea that every picture sub-region is homogeneous enough that the transformation between them can be discerned only by discontinuity. EAC are closely tied to edge-based segmentation. The regularity component, which specifies the shape of contours, and the edge detection component, which draws the contour toward the edges, are the two main components of the EAC models.

The edge-based active contour was implemented using the following steps:

i. Load the flooded satellite image: Load the required flooded satellite image that needs to be segmented.

ii. Preprocess the image: Preprocess the image to remove noise, improve contrast, and enhance the edges. This was done using adaptive thresholding.

iii. Initialize the contour: Initialize the contour as a closed curve that roughly encloses the flooded area. This was done automatically using thresholding.

iv. Compute the edge map: Compute the edge map or gradient map of the preprocessed image. This was done using the Canny gradient operator.

v. Compute the external energy: Compute the external energy using the edge map to attract the contour towards the edges of the flooded area.

vi. Compute the internal energy: Compute the internal energy based on the curvature, length, and other geometric properties of the contour to regularize the contour and prevent it from deforming excessively.

vii. Evolve the contour: Evolve the contour iteratively by minimizing a cost function that combines the external and internal energies. The contour is moved towards the edges of the flooded area while minimizing the internal energy to ensure that it remains smooth and well-behaved.

viii. Repeat until convergence: Repeat the process of computing the external and internal energies and evolving the contour until convergence is reached, typically when the change in contour position falls below a predefined threshold.

ix. Extract the segmented flooded area: Once the contour has converged, extract the flooded area by masking the pixels inside the contour.

### 3.3.2 Region-based active contour (RAC)

RAC techniques determine the optimal energy for which the model matches the picture the best based on data gathered from sub-regions. RAC models work better for photographs with weak edges and corners because they use a specific area attribute to direct the movement of the active contour rather than the image gradient to find each object of interest. Furthermore, RAC model is less affected by the position of original contours. Without respect to the location of the original contours, a RAC can detect inner borders. Independent segmentation is possible because to the use of pre-defined beginning contours.

The following steps provide a detailed description of how the images were analysed and segmented using the Region-based Active Contour algorithm:

i. Initialize the contour as a closed curve around the object of interest.

ii. Define the energy function that represents the trade off between the image intensity inside and outside the curve, and this energy function should be minimized to find the optimal contour.

iii. Iterate until convergence by calculating the gradient of the energy function with respect to the contour as it moves in the direction of the negative gradient.

iv. Assign each pixel in the image to either the inside or outside region of the contour based on which region has the lower energy.

v. Re-calculate the energy function using the updated inside and outside regions.

vi. Out put the final contour as a result of the algorithm.

A diagram of the RAC technique used is shown in Fig. 3.5.

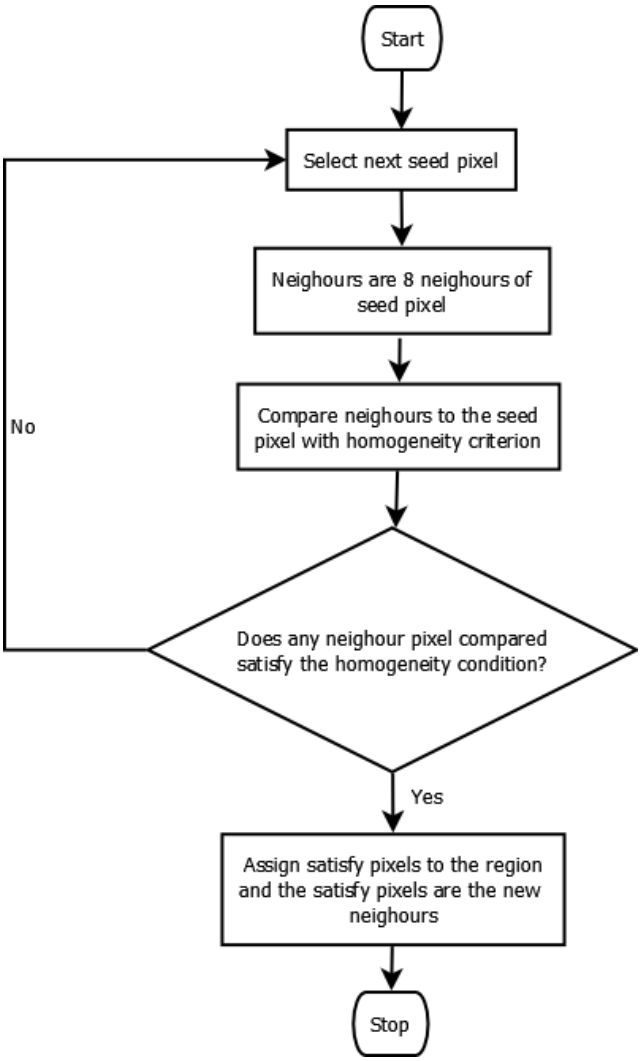


Figure 3.5 RAC segmentation procedure

### 3.3.3 Colour thresholding (CT) image segmentation

Colour thresholding is an image segmentation technique that involves separating objects or regions in an image based on their colour or colour range. This method involves choosing a threshold value for one or more of the image's colour channels, and then assigning a particular colour or label to each pixel or group of pixels based on whether or not their colour value falls within the threshold range. It is particularly useful for images with distinct and uniform colour regions, such as those obtained from

microscopy, medical imaging, or satellite imagery. Colour thresholding can be implemented using various colour spaces, such as RGB, HSL, HSV, and Lab, depending on the application and the type of colour information available in the image. For all types of photographs, a single-colour space cannot produce adequate results since segmentation outcomes depend on the chosen colour space. In this study the Hue, Saturation, Value (HSV) colour space for used to segment the colour photos.

A detailed explanation of the steps taken to anaylse and segment the satellite images using only the CT method in MATLAB is as follows:

i. The satellite images was converted to the appropriate colour space, which is HSV.
ii. The next step was the identification of the specific colour range that corresponds to the flooded areas in the image. This was done automatically using the adaptive thresholding histogram-based method.
iii. The colour thresholding was applied to the colour channels of the image by selecting a threshold value or range that separates the pixels of interest (flooded areas) from the background or other pixels. For instance, the flooded area were brown in colour, and a threshold value that captures the brown pixels in the image was selected.
iv. The thresholded image was then converted to a binary mask, where the pixels that meet the threshold criteria are assigned a value of 1, and the rest are assigned a value of 0.
v. The binary mask was post-processed to refine the segmentation results and remove any noise or artifacts using the MATLAB built in filter bwareafilt.

Finally the binary mask was used to mask the rgb image to produce the final segmented image.

### 3.3.4 K-means Clustering (KC) Segmentation

A technique for classifying a set of data into groups is called clustering. KC is one of the most often used techniques. K-means clustering is a popular unsupervised machine learning algorithm used for image segmentation. K-means clustering can be used to group similar pixels in an image into clusters based on their colour, texture, or other features, thereby facilitating the segmentation process. A collection of data is divided into k number of data categories in KC. It divides a given set of data into k different clusters. The KC algorithm has two features. The first stage involves finding the k centroid, and the second level involves moving each point to the cluster with the centroid that is closest to the data point. One of the most used methods for determining the distance to the closest centroid is the Euclidean distance. After clustering is accomplished, the elements in the group with the smallest Euclidean distance are assigned. This is done by recalculating the new cluster centre, creating a new Euclidean distance between each centre and each data point based on that centroid. Using the unsupervised KC approach, the interest area is also separated from the backdrop. The algorithm for k-means image segmentation is given in Table 3.1

**Table 3. 3 K-means segmentation algorithm**

**Input:** Image (I), with □ = {□$_1$, □$_2$, … , □$_□$} pixels

□ = {□$_1$, □$_2$, … , □$_□$} number of clusters

**Output:** Segmented image with K clusters

1. Start
2. Place each pixel into any cluster at random.
3. Calculate the range between each pixel and the. centroid C= {□$_1$, □, … , □$_□$}

□ = ∑$^{□}_{□-1}$ ∑$_{□□}$ ‖□$_{□}$ − □$_{□}$‖$^2$; □$_□$ ∈

Where ‖. ‖ denotes the Euclidean norm, □$_□$ = mean of all pixels in kth cluster

4. Reassign the pixel $\square$ to the cluster $\square$ Iff $\|\square - \square\|^2 \leq \|\square - \square\|; 1 \leq \square \leq \square$
5. Till no more assignments are made, repeat the previous processes.
6. End

The following steps provide a full explanation of how to analyse and segment images using the k-means clustering method:

i. Firstly preprocess the image by removing any noise or artifacts that may interfere with the clustering results. This was done using colour space conversion.

ii. Select the number of clusters, k that will be used for the segmentation. The k was selected manually as the number of k used was 3. This final k selection was done after experimenting ith various k values.

iii. Initialize the k-means clustering algorithm with the desired number of clusters and an initial set of centroid points.

iv. Assign each pixel in the image to the closest cluster centroid based on their colour or feature similarity. This was done using the Euclidean distance metric.

v. Recalculate the centroid values based on the new cluster assignments. This was donee using the mean values of the pixels in each cluster.

vi. Repeat steps 4 and 5 until the cluster assignments no longer change significantly, or a predetermined convergence criterion is met.

vii. Convert the clustered image to a binary mask, where the pixels that belong to the flooded areas are assigned a value of 1, and the rest are assigned a value of 0. This was done by thresholding the distance or similarity values obtained from the clustering algorithm.

viii. The binary mask was post-processed to refine the segmentation results and remove any noise or artifacts using the MATLAB built in filter bwareafilt.

Finally the binary mask was used to mask the rgb image to produce the final segmented image.

### 3.3.5 Colour-based K-means Clustering (Colour-based KC) Image Segmentation

The hybridization of colour thresholding and k-means clustering for segmentation involves combining the advantages of both techniques to achieve improved segmentation results. A block diagram of the proposed coloured-based KC segmentation is illustrated in Figure 3.6.

A block diagram of the proposed coloured-based KC segmentation is illustrated in Figure 3.6.

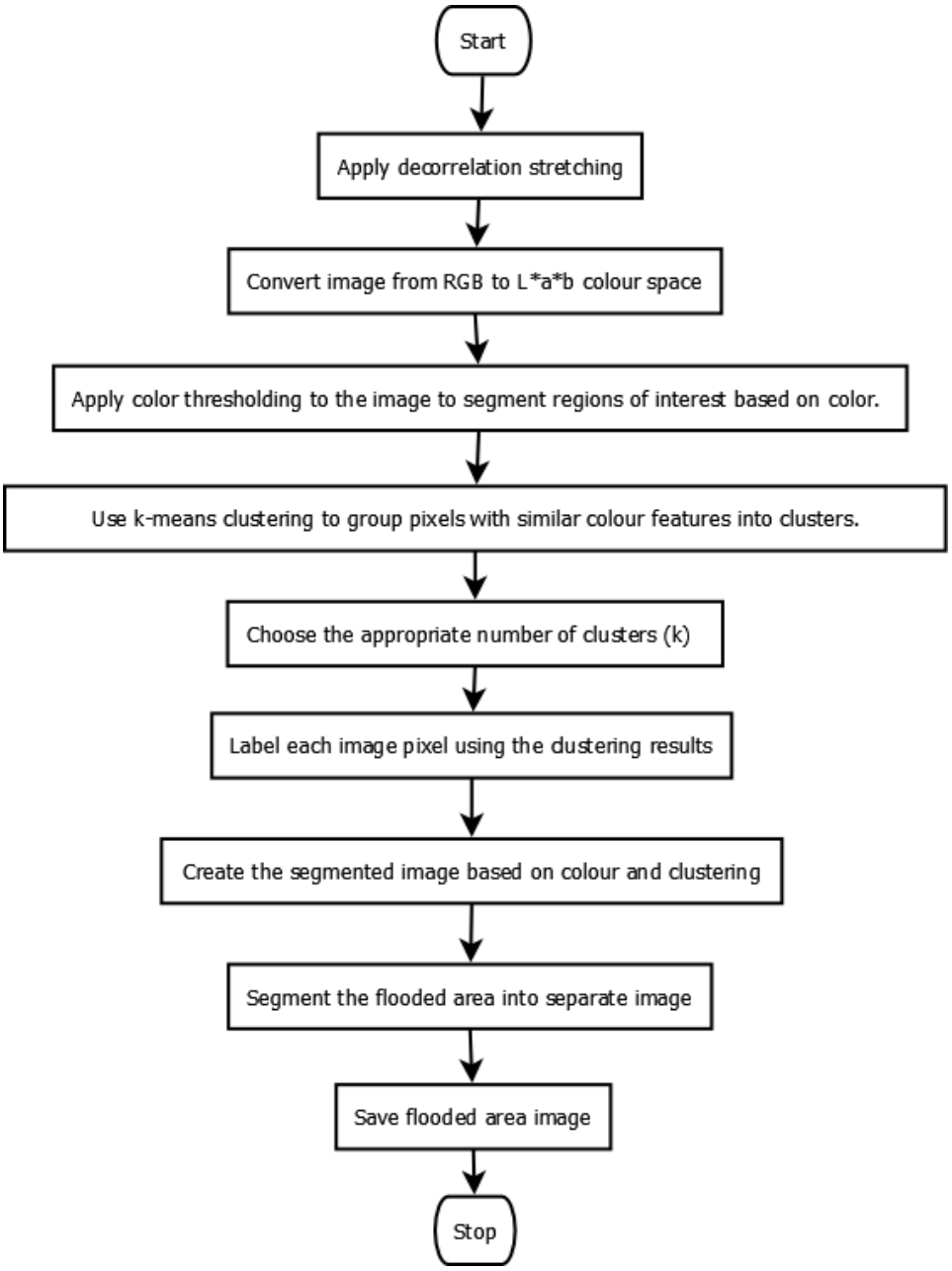


Figure 3.6 Coloured-based KC segmentation

The pseudocode of the proposed coloured-based k-means clustering segmentation as shown in Figure 3.6 is represented in Table 3.2:

**Table 3. 2 Pseudocode for proposed Colour-based K-means clustering segmentation**

The following is a pseudocode of the segmentation procedure:

Start

Step 1: Read the image in JPEG, PNG, GIF, and several image formats

Step 2: Apply Image Decorrelation stretching to improve the colour partition of the image with substantial band-band correlation.

Step 3: Convert enhanced image from RGB to L*a*b* colour space.

A luminance layer 'L*', a chromaticity layer 'a*' denotes where colour lies along its red-green plane, and a chromaticity level 'b*' specifies where colour lies along the blue-yellow plane making up the L*a*b* space. All of the colour information is contained in the 'a*' and 'b*' layers.

Step 4: Categorise the colours in the 'a*b*' plane utilising K-Means Clustering.

A technique for dividing up groups of objects is clustering. Each object is treated as possessing a location in space when using K-means clustering. It locates partitions so objects in each cluster are as close to one another and as far away from one another as possible. In order to use K-means clustering, you must define the number of clusters to be divided into as well as a distance metric to determine how near two items are to one another. Your objects are pixels with values of 'a*' and 'b*' since colour information resides in the 'a*b*' space. Utilizing the Euclidean distance metric, group the items into three clusters using K-means.

Step 5: Using the results of the clustering, label each pixel in the image.

K-means produces an index matching to a cluster for each object in our input. Give the cluster index for each pixel in the image.

Step 6: Create Images that Segment the Image by Colour.

Three photos will be produced as a consequence of colour-based item separation using pixel labels.

Step 7: Detach the flooded area into separate images.

The cluster index comprising the flooded areas should then be determined

programmatically because K-means will not consistently provide the same cluster_idx value. The cluster centre value, which includes the mean "a*" and "b*" values for each cluster, can be used to achieve this.

Step 8: Save the flooded area segmented image.

The saved image is compared with the ground truth image for evaluation purposes.

End

## 3.4 Performance Metrics

### 3.4.1 Intersection-over-union (IoU, Jaccard index)

The Jaccard Index, often known as the Intersection-over-Union (IoU) metric, is among the most widely applied metrics in image segmentation. IoU is a measurement statistic that assesses the precision of an object detector on a certain dataset. The forecast is 100 percent accurate if the IoU prediction value is 1 (Rezatofighi *et al.*, 2019). The lower the IoU, the worse the prediction result. IoU is represented by Equation 3.1.

$$\frac{\text{Area of Overlap}}{\text{Area of Union}} \tag{3.1}$$

### 3.4.2 Dice similarity coefficient (DSC)

A statistical instrument that assesses similarity between two sets of data is the dice similarity coefficient. Equation 3.2 is used to represent DSC.

$$\square\square\square = \frac{2 * \text{ Area ofoverlap}}{\text{total number of pixels in both images}} \tag{3.2}$$

### 3.4.3 Boundary F1 score (BFS)

The BF score is used to evaluate if a point on the projected boundary matches the ground truth boundary by calculating the harmonic mean (F1-measure) of the precision and recall values and adding a distance error tolerance. The degree to which an object's

predicted border matches the actual boundary is indicated by its BF score. Equation 3.3 represents the BFS.

$$\text{BFS} = \frac{2\times\text{precision}\times\text{recall}}{\text{recall} + \text{precision}} \tag{3.3}$$

### 3.4.4 Precision

The ratio of the number of pixels on the predicted segmentation's border that are near enough to the ground truth segmentation's boundary to the length of the predicted boundary is used to calculate precision. In other words, precision is the percentage of true positives versus false positives in a detection. The precision is calculated using the formula in equation 3.4.

$$\text{Precision} = \frac{\text{True Positive}}{\text{True Positive} + \text{False Positive}} \tag{3.4}$$

### 3.4.5 Recall

Calculating the recall requires dividing the number of sites on the ground truth boundary that are sufficiently close to the projected segmentation boundary by the ground truth boundary's length. In other words, recall is the percentage of true positives discovered rather than missed. The recall is calculated using the formula in equation 3.5.

$$\text{Recall} = \frac{\text{True Positive}}{\text{True Positive} + \text{False Negative}} \tag{3.5}$$

Where True positive is the pixel classified correctly as X, false positive is the pixel classified incorrectly as X; True Negative is the pixel classified correctly as not X, and false negative is the pixel classified incorrectly as not X.

## 3.5 Summary of Technique Used

After completing the data collection process. The Histogram equalization and decorrelation stretching techniques were used to enhance the quality and features of the

images. After performing image enhancement, the next step was image segmentation. Four methods were used in this image segmentation phase, namely, colour thresholding, edge-based, region-based and the proposed coloured-based K-means clustering segmentation technique. Each enhanced image was used as input to all the four segmentation techniques. The segmented images resulting from each segmentation method is then evaluated against the ground truth images using precision, recall, IoU, DSC and BFS performance measure to assess the performance of each technique.

# CHAPTER FOUR

# 4.0 RESULTS AND DISCUSSION

## 4.1 Results

The results of applying the suggested approach and various other algorithms to the high-resolution satellite imagery acquired from Airbus intelligence, NASA Earth Observatory and MODP are shown in this chapter. A full discussion of each acquired result is presented in the discussion section of this chapter.

### 4.1.1 Experimentation Environment

MATLAB 2018a was used in carrying out the experimentation and result evaluation in this research work. MATLAB is an acronym for Matrix Laboratory, it has an interactive interface and all infrastructure in MATLAB is in matrix form. MATLAB provides a perfect environment with a rich library of functions which can be used for testing of image processing algotithims. MATLAB is the most widely used engineering program in several areas regarding engineering, calculations, simulation, image processing, and other functions. The system used to conduct this experiment was Windows 11, AMD Ryzen 9 processor, 64-bit operating system, 4 GB video card and 16 GB RAM.

### 4.1.2 Segmented Images

Experiments were conducted on five different image segmentation algorithms: Region-based active contour (RAC), Edge-based active contour (EAC), Colour Thresholding (CT), K-means Clustering and Colour-based K-means Clustering (colour-based KC) concerning flooded area identification and segmentation.

Images of the results obtained after performing Edge-based and coloured-based k-means clustering segmentation is shown from Figure 4.2 to Figure 4.7 . Each of these figures are explained in detailed in the discussion section.

Figure 4. 1 Orginal Satellite Flooded Image

Figure 4.1 shows a sample of the satellite flooded image. In the image the brown coloured objects is the flooded area which is the area of interest.

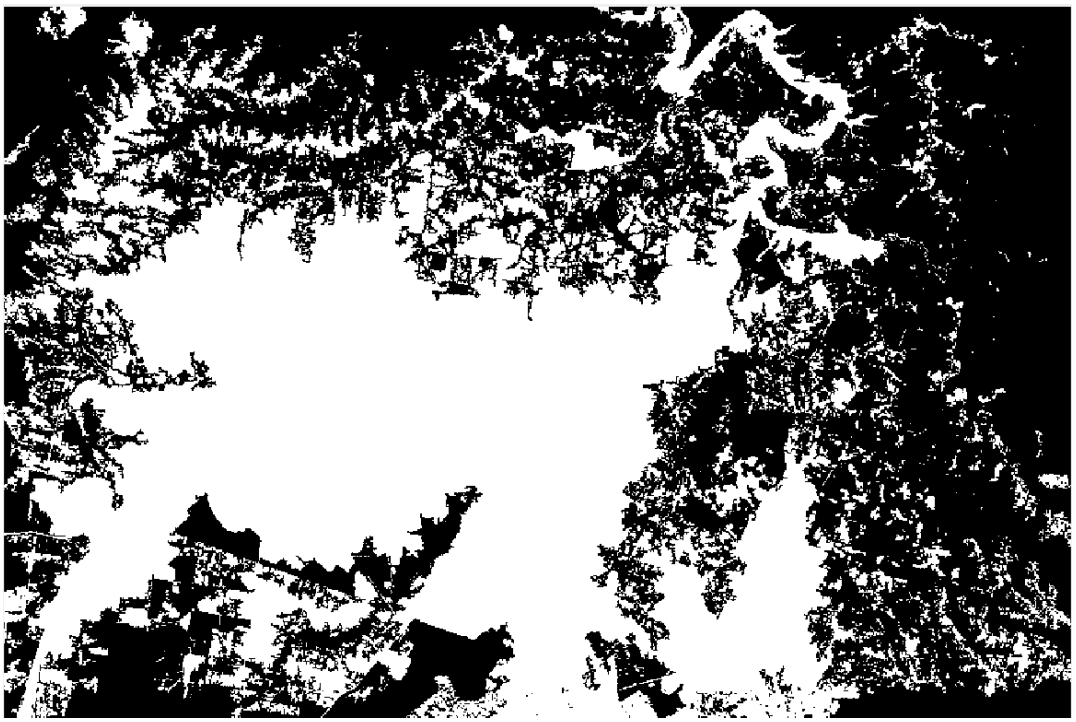

Figure 4. 2 Flooded Image mask after performing Edge-based Active contour

Figure 4.2 shows a mask of the original image after performing EAC segmentation. The white regions are the area of interest (flooded area) while the black regions are other areas which are outside the area of interest.

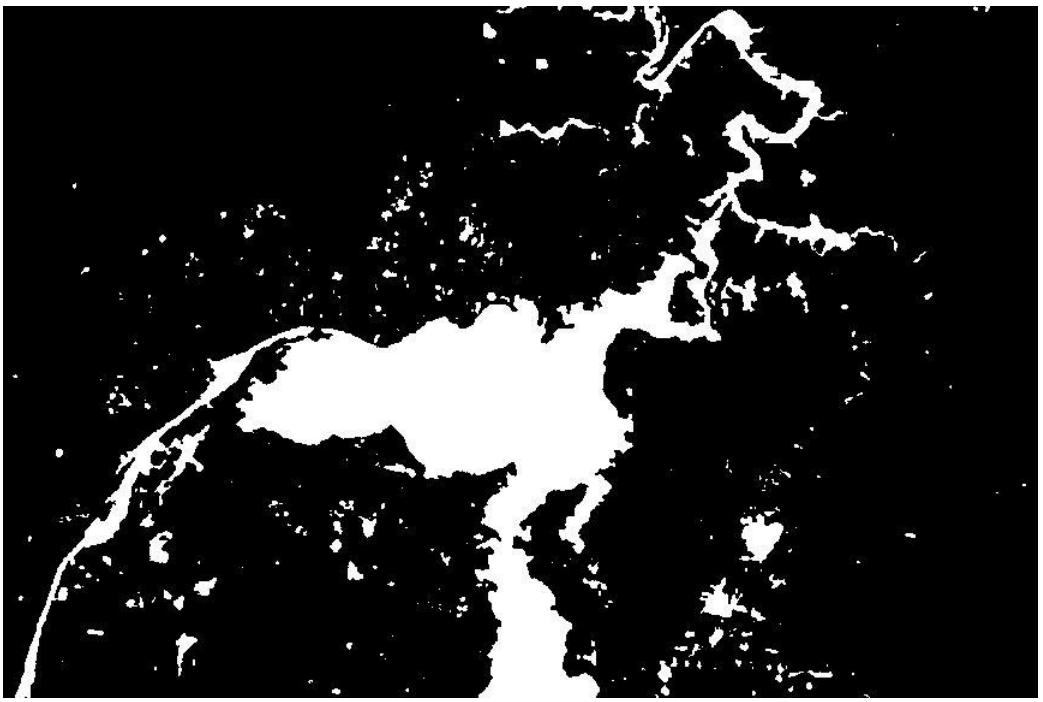

Figure 4. 3 Ground truth mask of the original image

Figure 4.3 shows the groud truth image mask. The white regions are the area of interest (flooded area) while the black regions are other areas which are outside the area of interest.

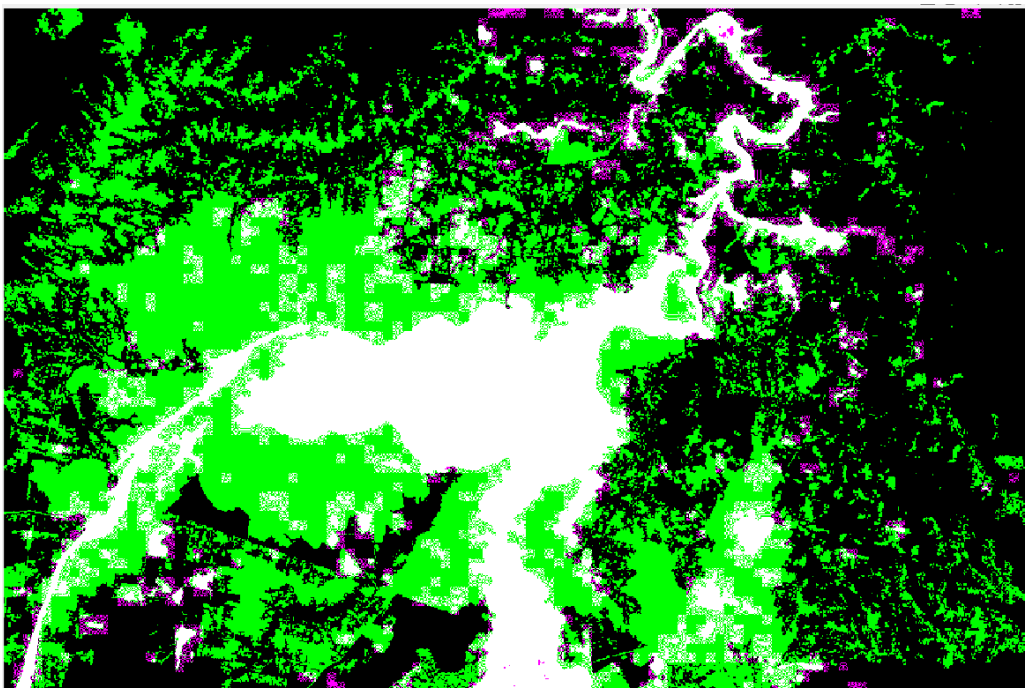

Figure 4. 4 After overlapping the ground truth mask with the Edge-based Active Contour mask

Figure 4.4 shows the overlaid image of the EAC mask and the ground truth mask. In the image the white and pink region shows the parts that was correctly segmented by the EAC model while the green region shows the wrongly segmented regions.


Figure 4. 5 First cluster after performing colour-based k-means clustering

Figure 4.5 is the first cluster which consist of buildings, roads and various infrastructure. The colours in this cluster are high contrast dark green mixed with gold.

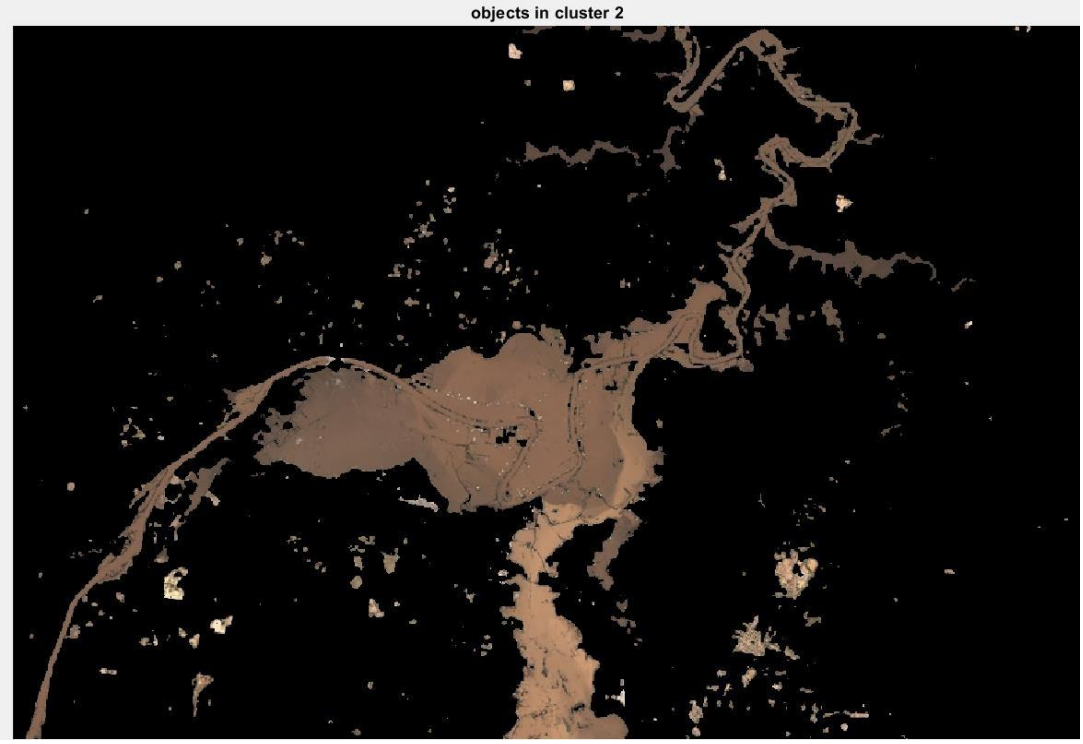


Figure 4. 6 Second cluster after performing colour-based k-means clustering

Figure 4.6 is the second cluster which consist of the flooded area which is the area of interest. It can be seen that the flooded area is brownish in colour.

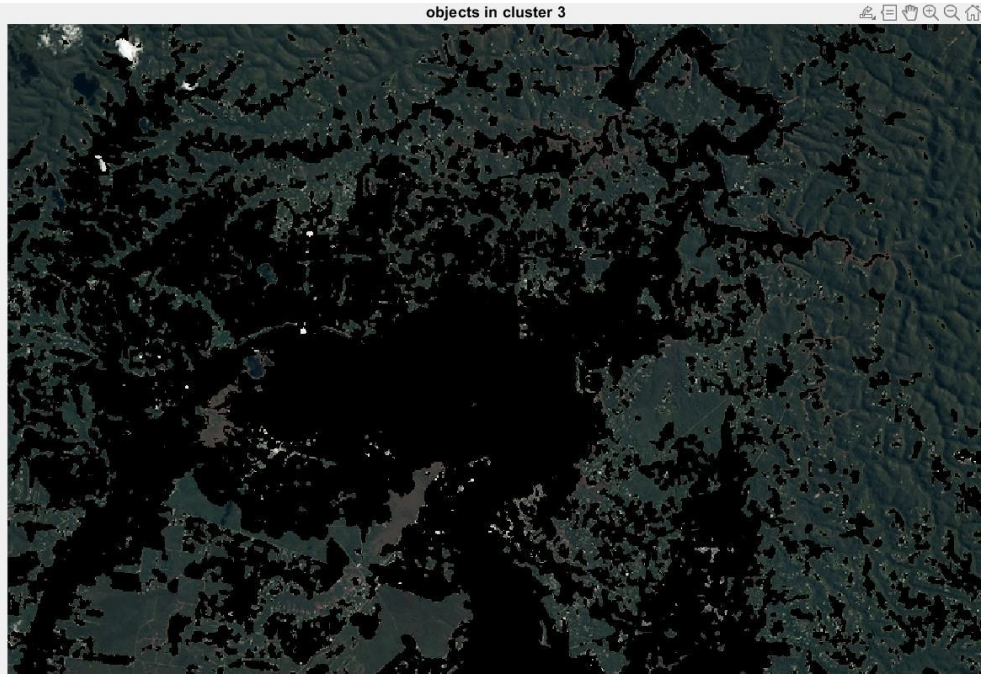


Figure 4. 7 Third cluster after performing colour-based k-means clustering

Figure 4.7 is the third cluster which consist of vegetations. It can be seen that the cluster are made up of greenish colour.

### 4.1.3 Segmentation Model Performance

The experiment was conducted on 24 satellite images. To avoid a cumbersome report, Table 4.1 shows the result obtained for six satellite images and the average performance of the five segmentation methods on these six images is also reported.

**Table 4. 1 Experimental result for flood detection on the satellite Images**

| Method | Images | Jaccard index | DSC | BFS | Precision | Recall |
|---|---|---|---|---|---|---|
| **Region-based** | Image1 | 0.5254 | 0.6889 | 0.5924 | 0.6427 | 0.5494 |
| | Image2 | 0.5949 | 0.7460 | 0.5235 | 0.6813 | 0.4251 |
| | Image3 | 0.6562 | 0.8148 | 0.6441 | 0.9055 | 0.4998 |
| | Image4 | 0.5352 | 0.7065 | 0.6956 | 0.8196 | 0.6043 |
| | Image5 | 0.4527 | 0.5215 | 0.6612 | 0.5986 | 0.7383 |
| | Image6 | 0.6466 | 0.8068 | 0.8122 | 0.8755 | 0.7575 |
| | **Average** | **0.5685** | **0.7141** | **0.6548** | **0.7539** | **0.5956** |
| **Edge-based** | Image1 | 0.3322 | 0.4770 | 0.3275 | 0.5900 | 0.2267 |
| | Image2 | 0.3649 | 0.5189 | 0.3252 | 0.5945 | 0.2239 |

| | | | | | | |
|---|---|---|---|---|---|---|
| | Image3 | 0.3694 | 0.5245 | 0.5561 | 0.7180 | 0.4538 |
| | Image4 | 0.4378 | 0.6050 | 0.4511 | 0.7985 | 0.3143 |
| | Image5 | 0.3072 | 0.4432 | 0.3347 | 0.4022 | 0.2866 |
| | Image6 | 0.4691 | 0.6316 | 0.4849 | 0.8979 | 0.3321 |
| | **Average** | **0.3801** | **0.5333** | **0.4133** | **0.6669** | **0.3062** |
| **Colour thresholding segmentation** | Image1 | 0.6594 | 0.7948 | 0.9266 | 0.9046 | 0.9496 |
| | Image2 | 0.6646 | 0.7985 | 0.9311 | 0.9047 | 0.9591 |
| | Image3 | 0.7125 | 0.8785 | 0.8623 | 0.9892 | 0.7643 |
| | Image4 | 0.8764 | 0.9313 | 0.9730 | 0.9977 | 0.9495 |
| | Image5 | 0.8050 | 0.8539 | 0.8859 | 0.9190 | 0.8551 |
| | Image6 | 0.6173 | 0.7888 | 0.8042 | 0.8863 | 0.7361 |
| | **Average** | **0.7225** | **0.8410** | **0.8972** | **0.9336** | **0.8690** |
| **K-means clustering** | Image1 | 0.6631 | 0.8344 | 0.9383 | 0.9384 | 0.9278 |
| | Image2 | 0.6559 | 0.8023 | 0.9376 | 0.9203 | 0.9408 |
| | Image3 | 0.7198 | 0.8932 | 0.8444 | 0.9833 | 0.7347 |
| | Image4 | 0.8954 | 0.9388 | 0.9561 | 0.9893 | 0.9432 |
| | Image5 | 0.7967 | 0.8706 | 0.8902 | 0.9239 | 0.8711 |
| | Image6 | 0.6512 | 0.8258 | 0.8443 | 0.9189 | 0.8305 |
| | **Average** | **0.7304** | **0.86085** | **0.90182** | **0.9457** | **0.8746** |
| **Colour-based K-means** | Image1 | 0.7946 | 0.9457 | 0.9333 | 0.9504 | 0.9169 |
| | Image2 | 0.6424 | 0.8143 | 0.9527 | 0.9647 | 0.9409 |
| | Image3 | 0.7422 | 0.9032 | 0.8228 | 0.9890 | 0.7044 |
| | Image4 | 0.9150 | 0.9539 | 0.9468 | 0.9787 | 0.9169 |
| | Image5 | 0.7789 | 0.9333 | 0.8920 | 0.8991 | 0.8850 |
| | Image6 | 0.8664 | 0.9498 | 0.9315 | 0.9304 | 0.9323 |
| | **Average** | **0.7899** | **0.9167** | **0.9132** | **0.9521** | **0.8827** |

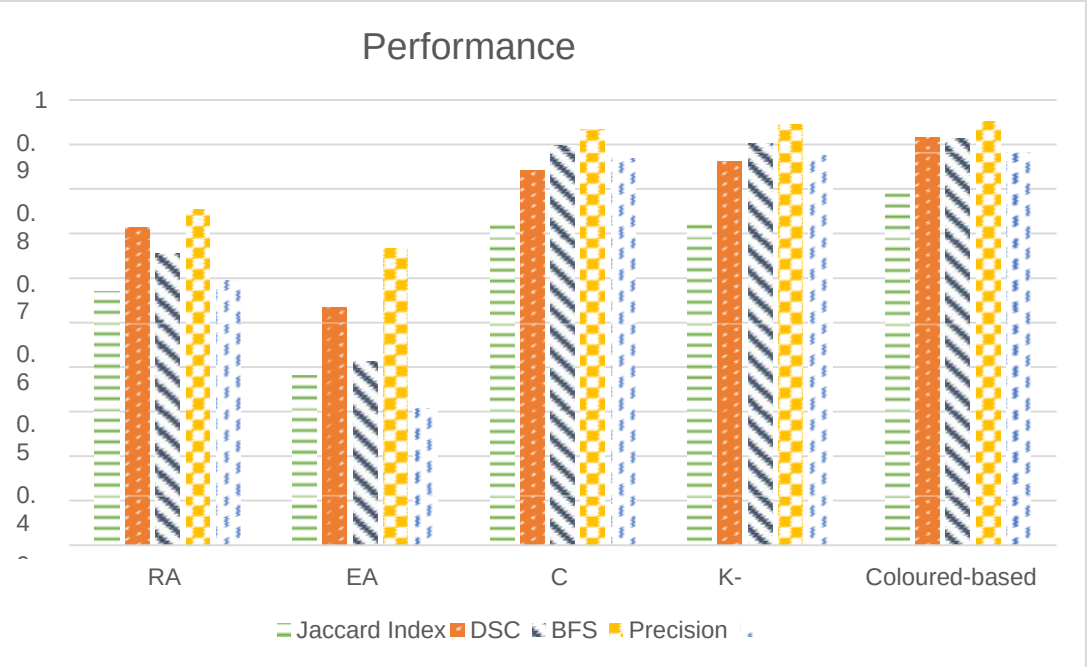


Figure 4.8 Performance assessment of five image segmentation techniques

Figure 4.8 is a column chart with different colour patterns showing the comparative performance of all the five models used in this study. The values used in the chart are the same as the values in Table 4.1.

## 4.2 Discussion

This section provides a detailed discussion of all the results (images, table, chart) presented in the results section of this chapter.

Table 4.1 demonstrates that the proposed coloured-based K-means clustering method generated the best accuracy on the flooded area dataset, with an average Jaccard index of 0.7899, compared to 0.7304, 0.7225, 0.3801, and 0.5685 respectively, for K-means, CT, EAC, and RAC. The second best performing model was the k-means clustering technique with jaccard index of 0.7304, DSC of 0.86085, precision of 0.9457 and recall of 0.8746. The k-means clustering technique outperformed the CT technique, which had a DSC of 0.8410, and the RAC technique had a DSC of 0.7141. The EAC approach has the lowest DSC value of 0.5333, indicating that the ground truth and EAC segmentation

are not very similar. However, 95.21% of the points detected by the coloured-based k-means method were true positive predictions rather than false positives. Furthermore, CT detects a high percentage of actual positive predictions rather than false positives, with a precision of 0.9336. The EAC approach produced the least precision (0.6669), followed by the RAC technique (0.7539).

When the five approaches were compared using the BFScore performance metric, the coloured-based k-means clustering came out on top with a score of 0.9132, followed by k-means clustering with 0.90182, CT with 0.8972, RAC with 0.6548, and EAC with 0.4133. Table 4.1 also reveals that the proposed coloured-based k-means clustering has a high recall value of 0.8827, implying that the number of right positive predictions made from all the positive predictions is better than k-means, CT, EAC, and RAC, which have recall values of 0.8746, 0.8690, 0.3062, and 0.5956, respectively.

After segmenting all 24 photos, coloured-based KC achieved the best overall performance, with a Jaccard Index of 0.8234, a DSC of 0.9234, a precision of 0.9589, a recall of 0.9078, and a BFscore of 0.9327. The k-means clustering was the second best after coloured-based KC which has a Jaccard index of 0.7683, DSC of 0.8998, the precision of 0.9479, recall of 0.8938, and BFscore of 0.9188, is the next method with good performance. The CT, which has a Jaccard index of 0.7456, DSC of 0.8690, the precision of 0.9465, recall of 0.8877, and BFscore of 0.9162, is the next method with good performance after k-means clustering. With a Jaccard index of 0.3957, DSC of 0.5555, the precision of 0.6578, recall of 0.3111, and BFscore of 0.4224, EAC performed the worst. On the 24 satellite pictures, RAC obtained an average Jaccard index of 0.5865, DSC of 0.7290, precision of 0.7783, recall of 0.6242, and BFscore of 0.6928. Table 4.2 shows a comparison of the best-performing method, coloured-based KC, with previous works.

### 4.3 Comparison with Related Works

A comparison of the coloured-based KC segmentation, Multi$^3$Net, and FCNN is shown in Table 4.2.

**Table 4. 2 Comparison of proposed Colour-based KC with related works**

| Method | Precision (%) | Recall (%) | BFscore (%) | Jaccard Index (%) |
|---|---|---|---|---|
| Fully convolutional neural network (FCNN) (Nemni *et al*., 2020) | 82 | 97 | 89 | - |
| Multi$^3$Net (Rudner *et al*., 2019) | - | - | - | 79.9 |
| Colour Based K-means clustering (proposed technique) | 95.9 | 90.8 | 93.3 | 82.3 |

A comparison of the coloured-based KC segmentation, Multi$^3$Net, and FCNN is shown in Table 4.2.

Table 4.2 presents a comparative analysis of the proposed method with existing works. This comparison was based on various performance metrics like precision, recall, BFscore and Jaccard Index. In comparison to Multi$^3$Net with Jaccard Index of 79.9% and Fully convolutional neural networks with a precisison of 82%, recall of 97% and BFscore of 89, the proposed coloured-based K-means clustering method achieved superior precision of 95.9%, recall of 90.8%, BFscore of 93.3%, and Jaccard index of 82.3%.

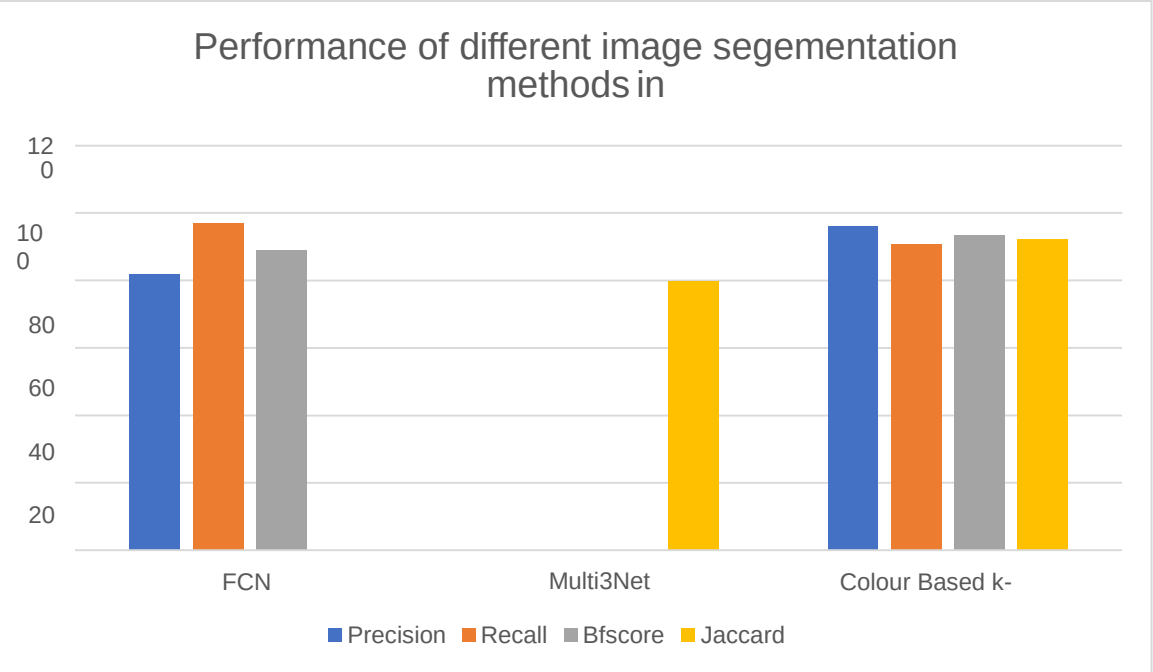


Figure 4.9 Comparison of Coloured-based KC with related works

Figure 4.9 is a chart representing the performance of the proposed approach in comparison with previous works as shown in Table 4.2. From the diagram it can be seen that only the Jaccard Index was used to measure the Multi$^3$Net technique while the FCNN was measured using precision, recall and BF score.

# CHAPTER FIVE

# 5.0 CONCLUSION AND RECOMMENDATION

## 5.1 Conclusion

This research have successfully achieved the three main objectives. Firstly, flood satellite image dataset was collected from Airbus Intelligence, NASA Earth Observatory and Maxar Open Data Program. This dataset was essential in providing us with the necessary information and images needed to develop and test our image segmentation technique. Secondly, the colour threshold-based and K-means clustering image segmentation techniques was successfully hybridized to create a novel flood detection technique. The hybrid technique was effective in segmenting the flooded areas of the satellite images accurately. This technique can be applied to various satellite images to detect floods and aid in disaster management.

Lastly, the performance of the proposed technique was evaluated using precision, recall, Intersection-over-Union, Boundary F1 Score and dice similarity coefficient. The proposed colour-based KC technique obtained precision of 95.9%, recall of 90.8%, BFS of 93.3%, Jaccard index of 82.34% and DSC of 92.3%. The results obtained showed that our technique performed better than existing techniques in detecting and segmenting flooded areas in satellite images.

In conclusion, the hybridisation of both colour threshold-based and K-means clustering image segmentation techniques has proven to be an effective method for flood detection in satellite imagery. This study has provided valuable insight into the use of image segmentation techniques in detecting and managing natural disasters such as floods. The results obtained can be applied in real-world scenarios to help in disaster management and recovery efforts.

## 5.2 Recommendation

The study made use of only five image segmentation techniques for flood identification on satellite imagery. For future work, the performance of more segmentation methods such as fuzzy logic and watershed segmentation methods on flood satellite images can be analysed. In addition, the performance of the five analysed techniques can be tested on other satellite imagery with different scenarios like vegetation, hurricanes, and buildings.

## 5.3 Contribution to Knowledge

This study contributes to knowledge as follows:

i. Hybridization of colour threshold-based and K-means clustering image segmentation techniques for flood detection in satellite imagery, which provided more accurate and efficient results compared to using either technique alone.

The hybrid technique to be applied to other types of imagery beyond flood detection, such as object recognition and medical image analysis.

## REFERENCES


Abdulateef, S., & Salman, M. (2021). A Comprehensive Review of Image Segmentation Techniques. *Iraqi Journal for Electrical and Electronic Engineering*, *17*(2), 166–175. https://doi.org/10.37917/ijeee.17.2.18

Abera, K. A., Asce, S. M., Kalehiwot, N., Manahiloh, P. E., Asce, M., & Nejad, M. M. (2017). The Effectiveness of Global Thresholding Techniques in Segmenting Two-Phase Porous Media. *Construction and Building Materials*, *142*(2), 256–267. https://www.sciencedirect.com/science/article/pii/S0950061817304191

Adegun, A., Ogundokun, R., Asani, E. O., Adegun, A. A., Akande, N. O., Ogundokun, R. O., & Asani, E. O. (2018). Image Segmentation And Classification Of Large Scale Satellite Imagery For Land Use: A Review Of The State Of The Arts. *International Journal of Civil Engineering and Technology (IJCIET)*, *9*(11), 1534–1541. http://www.iaeme.com/IJCIET/index.asp1534http://www.iaeme.com/ijciet/issues.asp?JType=IJCIET&VType=9&IType=11http://www.iaeme.com/IJCIET/issues.asp?JType=IJCIET&VType=9&IType=11

Amato, G., Ciampi, L., Falchi, F., Gennaro, C., & Messina, N. (2019). Learning pedestrian detection from virtual worlds. *Lecture Notes in Computer Science (Including Subseries Lecture Notes in Artificial Intelligence and Lecture Notes in Bioinformatics)*, *11751 LNCS*, 302–312. https://doi.org/10.1007/978-3-030-30642-7_27/COVER/

Amit, S. N. K. B., Shiraishi, S., Inoshita, T., & Aoki, Y. (2016). Analysis of satellite images for disaster detection. *International Geoscience and Remote Sensing Symposium (IGARSS)*, *2016-November*, 5189–5192. https://doi.org/10.1109/IGARSS.2016.7730352

Arulmurugan, R., & Anandakumar, H. (2018). Region-based seed point cell segmentation and detection for biomedical image analysis. *International Journal of Biomedical Engineering and Technology*, *27*(4), 273–289. https://doi.org/10.1504/IJBET.2018.094296

Babu, K., Ravi, K. Y., & Sukanta Sabut. (2017, May 20). An Improved Watershed Segmentation by Flooding and Pruning Algorithm for Assessment of Diabetic Wound Healing. *2nd IEEE International Conference on Recent Trends in Electronics, Information & Communication Technology*.

Baek, J., Jeong, M. K., & Elsayed, E. A. (2022). Residual-Based Surface Segmentation for Monitoring Topographic Variations. *IEEE Transactions on Automation Science and Engineering*, *19*(1), 280–294. https://doi.org/10.1109/TASE.2020.3027810.

Baldevbhai, P. J., & Anand, R. S. (2012). ColourImage Segmentation for Medical Images using L*a*b* ColourSpace. *IOSR Journal of Electronics and Communication Engineering (IOSRJECE)*, *1*(2), 24–45. www.iosrjournals.orgwww.iosrjournals.org

Bartesaghi, A., Sapiro, G., & Subramaniam, S. (2005). An energy-based three-dimensional segmentation approach for the quantitative interpretation of electron tomograms. *IEEE Transactions on Image Processing*, *14*(9), 1314–1323. https://doi.org/10.1109/TIP.2005.852467

Basar, S., Ali, M., Ochoa-Ruiz, G., Zareei, M., Waheed, A., & Adnan, A. (2020). Unsupervised Colourimage segmentation: A case of RGB histogram based K-means clustering initialization. *PLOS ONE*, *15*(10), e0240015. https://doi.org/10.1371/JOURNAL.PONE.0240015

Basavaprasad, B., &Hegadi, R. S. (2014). A Survey on Traditional and Graph Theoretical Techniques for Image Segmentation Article in International Journal of Computer Applications · February. *International Journal of Computer Applications*, 38–46. https://www.researchgate.net/publication/274270045

Baswaraj, B. D., Govardhan, A., Premchand, P., Baswaraj α, D., Govardhan σ, A., &Premchand ρ, P. (2012). Active Contours and Image Segmentation: The Current State of the Art Active Contours and Image Segmentation The Current State of the Art Strictly as per the compliance and regulations of: Active Contours and Image Segmentation: The Current State of the Art. *Type: Double Blind Peer Reviewed International Research Journal Publisher: Global Journals Inc*, *12*.

Bezdek, J. (2011). Fuzzy C-means cluster analysis. *Scholarpedia*, Vol *6*(7), 2057. https://doi.org/10.4249/scholarpedia.2057

Bhadoria, P., Agrawal, S., & Pandey, R. (2020). Image segmentation techniques for remote sensing satellite images. *IOP Conference Series: Materials Science and Engineering*, *993*(1). https://doi.org/10.1088/1757-899X/993/1/012050

Bhargavi, K., & Jyothi, S. (2014). A Survey on Threshold Based Segmentation Technique in Image Processing. *International Journal of Innovation Research & Development*, *3*(12), 234–239. https://www.researchgate.net/publication/309209325

Bharodiya, A. K., &Gonsai, A. M. (2019). An improved edge detection algorithm for X-Ray images based on the statistical range. *Heliyon*, *5*(10), e02743. https://doi.org/10.1016/J.HELIYON.2019.E02743

Bilham, R. (2010). Lessons from the Haiti earthquake. *Nature 463*,878–879 (2010). https://doi.org/10.1038/463878a

Birchfield, S. T., Natarajan, B., & Tomasi, C. (2007). Correspondence as energy-based segmentation. *Image and Vision Computing*, *25*(8), 1329–1340. https://doi.org/10.1016/j.imavis.2006.08.001

Bradley, D., & Roth, G. (2007). Adaptive Thresholding Using the Integral Image. *Journal of Graphics Tools*, *12*(2), 13–21.

Bräunl, T., Feyrer, S., Rapf, W., & Reinhardt, M. (2001). Edge Detection. *Parallel Image Processing*, 27–32. https://doi.org/10.1007/978-3-662-04327-1_4

Brunsma, D. L., Overfelt, David., Picou, J. Steven., Bankston, C. L. (Carl L., Barnshaw, John., Bevc, Christine., Capowich, G. E., Clarke, Lee., Das, S. K., Donato, K. M., Dynes, R. R. (Russell R., Eargle, L. A., Elliott, J. R., Esmail, A. M., Frailing,

Kelly., Fussell, Elizabeth., Green, J. J., Haney, T. J., Harper, D. Wood., … Wright, Delmar. (2010). *The Sociology of Katrina : Perspectives on a Modern Catastrophe.* Rowman & Littlefield Publishers. https://books.google.gr/books?hl=el&lr=&id=qwJlp_yTmcAC&oi=fnd&pg=PA55&dq=crime+rate+katrina&ots=Fp546n9wQg&sig=E9s24utIifWS_22pSf_ul7ixUsc&redir_esc=y#v=onepage&q=crime%20rate%20katrina&f=false

Camilus, K. S., & Govindan, V. K. (2012). A Review on Graph Based Segmentation. *International Journal of Image, Graphics and Signal Processing*, *4*(5), 1–13. https://doi.org/10.5815/ijigsp.2012.05.01

Canny, J. (1986). A Computational Approach to Edge Detection. *IEEE Transactions on Pattern Analysis and Machine Intelligence*, *PAMI-8*(6), 679–698. https://doi.org/10.1109/TPAMI.1986.4767851.

CaporHrosik, R., Tuba, E., Dolicanin, E., Jovanovic, R., & Tuba, M. (2019). Brain image segmentation based on firefly algorithm combined with k-means clustering. *Studies in Informatics and Control*, *28*(2), 167–176. https://doi.org/10.24846/v28i2y201905

Cavallo, E., Powell, A., & Becerra, O. (2010). Estimating the direct economic damages of the earthquake in Haiti. *Economic Journal*, *120*(546). https://doi.org/10.1111/J.1468-0297.2010.02378.X

Celebi, M. E., &Kingravi, H. A. (2013). Deterministic Initialization of the K-Means Algorithm Using Hierarchical Clustering. *International Journal of Pattern Recognition and Artificial Intelligence*, *26*(7), 1250018. https://doi.org/10.1142/S0218001412500188

Celik, S., &Corbacioglu, S. (2010). Role of information in collective action in dynamic disaster environments. *Disasters*, *34*(1), 137–154. https://doi.org/10.1111/J.1467-7717.2009.01118.X

Cheng, H. D., Jiang, X. H., Sun, Y., & Wang, J. (2001). Colour image segmentation: advances and prospects. *Pattern Recognition*, *34*(12), 2259–2281. https://doi.org/10.1016/S0031-3203(00)00149-7

Chitade, A. Z. (2010). *Colour Based Image Segmentation using K-Means Clustering*. *International Journal of Engineering Science and Technology*, *2*(10), 5319–5325.

Ciecholewski, M. (2016). An edge-based active contour model using an inflation/deflation force with a damping coefficient. *Expert Systems with Applications*, *44*, 22–36. https://doi.org/10.1016/j.eswa.2015.09.013

Dhanachandra, N., Manglem, K., & Chanu, Y. J. (2015a). Image Segmentation Using K-means Clustering Algorithm and Subtractive Clustering Algorithm. *Procedia Computer Science*, *54*, 764–771. https://doi.org/10.1016/j.procs.2015.06.090

Dhanachandra, N., Manglem, K., & Chanu, Y. J. (2015b). Image Segmentation Using K-means Clustering Algorithm and Subtractive Clustering Algorithm. *Procedia Computer Science*, *54*, 764–771. https://doi.org/10.1016/J.PROCS.2015.06.090

Dhanachandra, N., Manglem, K., & Chanu, Y. J. (2015c). Image Segmentation Using K-means Clustering Algorithm and Subtractive Clustering Algorithm. *Procedia Computer Science*, *54*, 764–771. https://doi.org/10.1016/j.procs.2015.06.090

Dimauro, G., & Simone, L. (2020). Novel Biased Normalized Cuts Approach for the Automatic Segmentation of the Conjunctiva. *Electronics 2020, Vol. 9, Page 997*, *9*(6), 997. https://doi.org/10.3390/ELECTRONICS9060997

Dorninger, P., & Pfeifer, N. (2008). A comprehensive automated 3D approach for building extraction, reconstruction, and regularization from airborne laser scanning point clouds. *Sensors*, *8*(11), 7323–7343. https://doi.org/10.3390/S8117323

Dubey, S. K., & Vijay, S. (2018). A Review of Image Segmentation using Clustering Methods. *International Journal of Applied Engineering Research*, *13*(5), 2484–2489. http://www.ripublication.com

Eriksson, A., Olsson, C., & Kahl, F. (2010). Normalized Cuts Revisited: A Reformulation for Segmentation with Linear Grouping Constraints. *Journal of Mathematical Imaging and Vision 2010 39:1*, *39*(1), 45–61. https://doi.org/10.1007/S10851-010-0223-5

Fawwaz, I., Zarlis, M., Suherman, & Rahmat, R. F. (2018). The edge detection enhancement on satellite image using bilateral filter. *IOP Conference Series: Materials Science and Engineering*, *308*(1). https://doi.org/10.1088/1757-899X/308/1/012052

Freedman, D., & Zhang, T. (2005). Interactive graph cut based segmentation with shape priors. *Proceedings - 2005 IEEE Computer Society Conference on Computer Vision and Pattern Recognition, CVPR 2005*, *I*, 755–762. https://doi.org/10.1109/CVPR.2005.191

Freeman, D., Reeve, S., Robinson, A., Ehlers, A., Clark, D., Spanlang, B., & Slater, M. (2017). Virtual reality in the assessment, understanding, and treatment of mental health disorders. In *Psychological Medicine* (Vol. 47, Issue 14, pp. 2393–2400). Cambridge University Press. https://doi.org/10.1017/S003329171700040X

Ganguly, S., Bose, D., & Konar, A. (2014). Clustering using vector membership: An extension of the Fuzzy C-Means algorithm. *2013 5th International Conference on Advanced Computing, ICoAC 2013*, 27–32. https://doi.org/10.1109/ICOAC.2013.6921922

Gao, W., Yang, L., Zhang, X., & Liu, H. (2010). An improved Sobel edge detection. *Proceedings - 2010 3rd IEEE International Conference on Computer Science and Information Technology, ICCSIT 2010*, *5*, 67–71. https://doi.org/10.1109/ICCSIT.2010.5563693

Geetha, M., Megha, M., Sarika, A. S., Mauktha, M., & Sethuraman, R. N. (2017). Detection and Estimation of the Extent of Flood from Crowd Sourced Images. *International Conference on Communication and Signal Processing*, 603–608.

Ghosh, S., & Dubey, S. K. (2013). Comparative Analysis of K-Means and Fuzzy C-Means Algorithms. *IJACSA) International Journal of Advanced Computer Science and Applications*, *4*(4). www.ijacsa.thesai.org

Guha-Sapir, D., Hoyois, P., & Below, R. (2015). *Annual Disaster Statistical Review 2014 The numbers and trends*. https://doi.org/10.13140/RG.2.2.10378.88001

Hagenmuller, P., Chambon, G., Lesaffre, B., Flin, F., & Naaim, M. (2013). Energy-based binary segmentation of snow microtomographic images. *Journal of Glaciology*, *59*(217), 859–873. https://doi.org/10.3189/2013JoG13J035

Hameed, I. M., Abdulhussain, S. H., &Mahmmod, B. M. (2021). Content-based image retrieval: A review of recent trends. *Taylor & Francis*, *8*(1), 1–37. https://doi.org/10.1080/23311916.2021.1927469

Haoran, L., Huiyuan, F., Xiaojun, H., & Liang, L. (2019). ESNET: Edge-based segmentation Network for Real-Time Semantic Segmentation in Traffic Scenes. *IEEE International Conference on Image Processing (ICIP): Proceedings*, 1855–1860.

Haripriya, S., & Nanmaran, R. (2022). Design and Development of Decorrelation Stretch Technique for Enhancing the Quality of Satellite Images with Improved MSE and UIQI in Comparison with Wiener Filter filter. *ECS Transactions*, *107*(1), 13279–13288. https://doi.org/10.1149/10701.13279ecst

Harrabi, R., &Braiek, E. ben. (2012). *Colourimage segmentation using multi-level thresholding approach and data fusion techniques: application in the breast cancer cells images*. https://doi.org/10.1186/1687-5281-2012-11

Hemalatha, R. J., Thamizhvani, T. R., Dhivya, A. J. A., Joseph, J. E., Babu, B., & Chandrasekaran, R. (2018). Active Contour Based Segmentation Techniques for Medical Image Analysis. In *Medical and Biological Image Analysis*. InTech. https://doi.org/10.5772/intechopen.74576

Hernández, D., Cecilia, J. M., Cano, J. C., & Calafate, C. T. (2022). Flood Detection Using Real-Time Image Segmentation from Unmanned Aerial Vehicles on Edge-Computing Platform. *Remote Sensing*, *14*(1). https://doi.org/10.3390/rs14010223

Iannizzotto, G., & Vita, L. (2000). Fast and accurate edge-based segmentation with no contour smoothing in 2-D real images. *IEEE Transactions on Image Processing*, *9*(7), 1232–1237. https://doi.org/10.1109/83.847835

Ibrahim, A., & El-Kenawy, E.-S. M. (2020). Image Segmentation Methods Based on Superpixel Techniques: A Survey. *Journal of Computer Science and Information Systems*, *1*(6), 1–10. www.jcsis.org/

Jamil, A. M. Saif, H. Hammad, M., & A. A. Alqubati, I. (2016). Gradient Based Image Edge Detection. *International Journal of Engineering and Technology*, *8*(3), 153–156. https://doi.org/10.7763/ijet.2016.v6.876

Jang, J. W., Lee, S., Hwang, H. J., & Baek, K. R. (2013). Global thresholding algorithm based on boundary selection. *International Conference on Control, Automation and Systems*, 704–706. https://doi.org/10.1109/ICCAS.2013.6703961

Jayapriya, P., & Hemalatha, S. (2019). Comparative Analysis Of Image Segmentation Techniques And Its Algorithm. *International Journal of Scientific & Technology Research*, *8*(10), 2209–2212. www.ijstr.org

Jerripothula, K. R., Cai, J., Lu, J., & Yuan, J. (2017). Object co-skeletonization with co-segmentation. *Proceedings - 30th IEEE Conference on Computer Vision and*

*Pattern Recognition, CVPR 2017, 2017-January,* 3881–3889. https://doi.org/10.1109/CVPR.2017.413

Jia, X., Lei, T., Du, X., Liu, S., Meng, H., & Nandi, A. K. (2020). Robust Self-Sparse Fuzzy Clustering for Image Segmentation. *IEEE Access*, *8*, 146182–146195. https://doi.org/10.1109/ACCESS.2020.3015270

Jiang, Y., Tong, G., Yin, H., & Xiong, N. (2019). A Pedestrian Detection Method Based on Genetic Algorithm for Optimize XGBoost Training Parameters. *IEEE Access*, *7*, 118310–118321. https://doi.org/10.1109/ACCESS.2019.2936454

Johnson, B. A., & Ma, L. (2020). Image segmentation and object-based image analysis for environmental monitoring: Recent areas of interest, researchers' views on the future priorities. In *Remote Sensing* (Vol. 12, Issue 11). MDPI AG. https://doi.org/10.3390/rs12111772

Juergens, C., & Meyer-Heß, M. F. (2021). Identification of construction areas from vhr-satellite images for macroeconomic forecasts. *Remote Sensing*, *13*(13). https://doi.org/10.3390/rs13132618

Kaissis, G. A., Makowski, M. R., Rückert, D., & Braren, R. F. (2020). Secure, privacy-preserving and federated machine learning in medical imaging. *Nature Machine Intelligence 2020 2:6*, *2*(6), 305–311. https://doi.org/10.1038/s42256-020-0186-1

Kaku, K. (2019). Satellite remote sensing for disaster management support: A holistic and staged approach based on case studies in Sentinel Asia. In *International Journal of Disaster Risk Reduction* (Vol. 33, pp. 417–432). Elsevier Ltd. https://doi.org/10.1016/j.ijdrr.2018.09.015

Kamalakannan, S., Gururajan, A., Sari-Sarraf, H., Long, R., &Antani, S. (2010). Double-edge detection of radiographic lumbar vertebrae images using pressurized open DGVF snakes. *IEEE Transactions on Biomedical Engineering*, *57*(6), 1325–1334. https://doi.org/10.1109/TBME.2010.2040082

Kang, W.-X., Yang, Q.-Q., & Liang, R.-P. (2009). The Comparative Research on Image Segmentation Algorithms; The Comparative Research on Image Segmentation Algorithms. *2009 First International Workshop on Education Technology and Computer Science*, *2*. https://doi.org/10.1109/ETCS.2009.417

Karanwal, S. (2021). Implementation of Edge Detection at Multiple Scales. *International Journal of Engineering and Manufacturing*,*1*, 1–10. https://doi.org/10.5815/ijem.2021.01.01

Kaur, M., & Goyal, P. (2013). A Review on Region Based Segmentation. *International Journal of Science and Research*, *4*, 2319–7064. www.ijsr.net

Kenneth, M. Ogbuka., Agushaka, J., &Oyefolahan, I. O. (2019). Overlapping Sickle Cells Detection and Separation using Marker-based watershed segmentation. *I-Manager's Journal on Image Processing*, *6*(4), 1. https://doi.org/10.26634/jip.6.4.16752

Khan, A., Garner, R., Rocca, M. la, Salehi, S., & Duncan, D. (2022). A Novel Threshold-Based Segmentation Method for Quantification of COVID-19 Lung

Abnormalities. *Signal, Image and Video Processing 2022*, 1–8. https://doi.org/10.1007/S11760-022-02183-6

Khan, A., Gupta, S., & Gupta, S. K. (2020). Multi-hazard disaster studies: Monitoring, detection, recovery, and management, based on emerging technologies and optimal techniques. *International Journal of Disaster Risk Reduction*, *47*, 101642. https://doi.org/10.1016/J.IJDRR.2020.101642

Khan, M., Chakraborty, S., Astya, R., &Khepra, S. (2019). Face Detection and Recognition Using OpenCV. *Proceedings - 2019 International Conference on Computing, Communication, and Intelligent Systems, ICCCIS 2019*, *2019-January*, 116–119. https://doi.org/10.1109/ICCCIS48478.2019.8974493

Khang, T. D., Tran, M. K., & Fowler, M. (2021). A novel semi-supervised fuzzy c-means clustering algorithm using multiple fuzzification coefficients. *Algorithms*, *14*(9). https://doi.org/10.3390/a14090258

Khattab, D., Ebied, H. M., Hussein, A. S., & Tolba, M. F. (2014). Colourimage segmentation based on different Colourspace models using automatic GrabCut. *Scientific World Journal*, *2014*. https://doi.org/10.1155/2014/126025

Knabb, R. D., Rhome, J. R., & Brown, D. P. (2005). *Tropical Cyclone Report: Hurricane Katrina*. Vol 159, 32-37

Kulkarni, N. (2012). ColourThresholding Method for Image Segmentation of Natural Images. *International Journal of Image, Graphics and Signal Processing*, *4*(1), 28–34. https://doi.org/10.5815/ijigsp.2012.01.04

Kumar, N. R., & Deb, S. K. K. (2010). Water-Body Area Extraction from High Resolution Satellite Images-An Introduction, Review, and Comparison. *International Journal of Image Processing (IJIP)*, *3*(6), 353–372.

Kumar V. A., & Mishra, A. (2012). ColourImage Enhancement Techniques: A Critical Review. *Indian Journal of Computer Science and Engineering (IJCSE)*, *3*(1), 39–45.

Kumar, A., Kaur, A., & Kumar, M. (2018). Face detection techniques: a review. *Artificial Intelligence Review 2018 52:2*, *52*(2), 927–948. https://doi.org/10.1007/S10462-018-9650-2

Kushwah, C. P., & Markam, K. (2021). Semantic Segmentation of Satellite Images using Deep Learning. *International Journal of Innovative Technology and Exploring Engineering (IJITEE)*, 2278–3075. https://doi.org/10.35940/ijitee.H9186.0610821

Lai, C. L., Yang, J. C., & Chen, Y. H. (2007). A Real Time Video Processing Based Surveillance System for Early Fire and Flood Detection. *Instrumentation and Measurement Technology Conference*.

Latif, A., Rasheed, A., Sajid, U., Ahmed, J., Ali, N., Ratyal, N. I., Zafar, B., Dar, S. H., Sajid, M., & Khalil, T. (2019). Content-based image retrieval and feature extraction: A comprehensive review. *Mathematical Problems in Engineering*, *2019*. https://doi.org/10.1155/2019/9658350

Lettieri, E., Masella, C., & Radaelli, G. (2009). Disaster management: Findings from a systematic review. *Disaster Prevention and Management: An International Journal*, *18*(2), 117–136. https://doi.org/10.1108/09653560910953207

Li, D., Cao, Y., Tang, X. S., Yan, S., & Cai, X. (2018). Leaf Segmentation on Dense Plant Point Clouds with Facet Region Growing. *Sensors* , *18*(11), 3625. https://doi.org/10.3390/S18113625

Liu, H., Fang, J., Zhang, Z., & Lin, Y. (2020). A Novel Active Contour Model Guided by Global and Local Signed Energy-Based Pressure Force. *IEEE Access*, *8*, 59412–59426. https://doi.org/10.1109/ACCESS.2020.2981596

Li, J., Lei, P., & Todorovic, S. (2018). Weakly Supervised Energy-Based Learning for Action Segmentation. *Computer Vision Foundation*. https://github.com/JunLi-

Liu, X., Deng, Z., & Yang, Y. (2019). Recent progress in semantic image segmentation. *Artificial Intelligence Review*, *52*(2), 1089–1106. https://doi.org/10.1007/S10462-018-9641-3/FIGURES/12

Liu, Z., Chen, B., & Zhang, A. (2020). Building segmentation from satellite imagery using U-Net with ResNet encoder. *Proceedings - 2020 5th International Conference on Mechanical, Control and Computer Engineering, ICMCCE 2020*, 1967–1971. https://doi.org/10.1109/ICMCCE51767.2020.00431

Lu, Y., Chen, Y., Zhao, D., & Chen, J. (2019). Graph-FCN for Image Semantic Segmentation. *Lecture Notes in Computer Science (Including Subseries Lecture Notes in Artificial Intelligence and Lecture Notes in Bioinformatics)*, *11554 LNCS*, 97–105. https://doi.org/10.1007/978-3-030-22796-8_11/COVER/

Lu, Z., Xu, H., & Liu, G. (2019). A Survey of Object Co-Segmentation. *IEEE Access*, *7*, 62875–62893. https://doi.org/10.1109/ACCESS.2019.2917152

Maini, R., & Aggarwal, H. (2010). *A Comprehensive Review of Image Enhancement Techniques*. *2*(3), 8–13. *Journal of Computing, Vol 2(3)*. https://doi.org/10.48550/arXiv.1003.4053

Manfré, L. A., Hirata, E., Silva, J. B., Shinohara, E. J., Giannotti, M. A., Paula Larocca, A. C., & Quintanilha, J. A. (2012). An Analysis of Geospatial Technologies for Risk and Natural Disaster Management. *ISPRS International Journal of Geo-Information*, *1*, 166–185. https://doi.org/10.3390/ijgi1020166

Maxar. (2021). *High-resolution Satellite Imagery*. Open Data Program. https://www.maxar.com/products/satellite-imagery

Mondal, A. (2019). Fuzzy energy based active contour model for multi-region image segmentation. *Multimedia Tools and Applications 2019 79:1*, *79*(1), 1535–1554. https://doi.org/10.1007/S11042-019-08207-7

Mueller, M., Segl, K., & Kaufmann, H. (2004). Edge- and region-based segmentation technique for the extraction of large, man-made objects in high-resolution satellite imagery. *Pattern Recognition*, *37*(8), 1619–1628. https://doi.org/10.1016/j.patcog.2004.03.001

Muhadi, N. A., Abdullah, A. F., Bejo, S. K., Mahadi, M. R., &Mijic, A. (2020). Image segmentation methods for flood monitoring system. *Water (Switzerland)*, *12*(6). https://doi.org/10.3390/w12061825

Mushtaq, M., Akram, M. U., Alghamdi, N. S., Fatima, J., & Masood, R. F. (2022). Localization and Edge-Based Segmentation of Lumbar Spine Vertebrae to Identify the Deformities Using Deep Learning Models. *Sensors*, *22*(4). https://doi.org/10.3390/s22041547

Nair, V. (2018). *Efficient Region and Edge Based Image Segmentation Technique*. https://www.researchgate.net/publication/353141926

NASA. (2021). *NASA Earth Observatory - Home*. Earth Observatory. https://earthobservatory.nasa.gov/

Nemni, E., Bullock, J., Belabbes, S., & Bromley, L. (2020). Fully convolutional neural network for rapid flood segmentation in synthetic aperture radar imagery. *Remote Sensing*, *12*(16). https://doi.org/10.3390/RS12162532

Ng, H. P., Ong, S. H., Foong, K. W. C., Goh, P. S., & Nowinski, W. L. (2006). Medical image segmentation using k-means clustering and improved watershed algorithm. *Proceedings of the IEEE Southwest Symposium on Image Analysis and Interpretation*, *2006*, 61–65. https://doi.org/10.1109/ssiai.2006.1633722

Padmasini, N., Umamaheswari, R., &Sikkandar, M. Y. (2018). State-of-the-art of level-set methods in segmentation and registration of spectral domain optical coherence tomographic retinal images. *Soft Computing Based Medical Image Analysis*, 163–181. https://doi.org/10.1016/B978-0-12-813087-2.00009-9

Park, S. W., & Lee, Y. W. (2019). *Detection of forest disaster using high-resolution satellite images with semantic segmentation*. 59. https://doi.org/10.1117/12.2532990

Patel, D., &Yerpude, A. (2018). Content based Image Retrieval: A Review. *International Journal of Engineering Research & Technology*, *3*(20). https://doi.org/10.17577/IJERTCONV3IS20029

Patel, K. B., Zalte, M. B., & Panchal, S. R. (2013). A Review: Machine vision and its Applications. *IOSR Journal of Electronics and Communication Engineering*, *7*(5), 72–77. www.iosrjournals.org

Patel, K. K., Kar, A., Jha, S. N., & Khan, M. A. (2012). Machine vision system: A tool for quality inspection of food and agricultural products. In *Journal of Food Science and Technology* (Vol. 49, Issue 2, pp. 123–141). https://doi.org/10.1007/s13197-011-0321-4

Patil, M. P., Ratnaparkhe, V. R., &Kakarwal, S. N. (2015). Adaptive Thresholding for Image Enhancement : Hardware Approach. *International Journal of Engineering Research & Technology (IJERT)*, *2*(3), 1–4. www.ijert.org

Peng, B., Al-Huda, Z., Xie, Z., & Wu, X. (2020). Multi-scale region composition of hierarchical image segmentation. *Multimedia Tools and Applications 2020 79:43*, *79*(43), 32833–32855. https://doi.org/10.1007/S11042-020-09346-Y

Peng, B., Zhang, L., & Zhang, D. (2013). A survey of graph theoretical approaches to image segmentation. *Pattern Recognition*, *46*(3), 1020–1038. https://doi.org/10.1016/J.PATCOG.2012.09.015

Pithadiya, K. J., Modi, C. K., & Chauhan, J. D. (2009). Comparison of optimal edge detection algorithms for liquid level inspection in bottles. *2009 2nd*

*International Conference on Emerging Trends in Engineering and Technology, ICETET 2009*, 447–452. https://doi.org/10.1109/ICETET.2009.55

Popescu, D., Ichim, L., & Stoican, F. (2018). Flooded Area Segmentation from UAV Images Based on Generative Adversarial Networks. *2018 15th International Conference on Control, Automation, Robotics and Vision, ICARCV 2018*, 1361–1366. https://doi.org/10.1109/ICARCV.2018.8581341.

Priyadharsini, R., & Sharmila, T. S. (2019). Object Detection in Underwater Acoustic Images Using Edge Based Segmentation Method. *Procedia Computer Science*, *165*, 759–765. https://doi.org/10.1016/j.procs.2020.01.015

Qianyu, F., #1, Z., Jindapetch, N., Duangsoithong, R., &Buranapanichkit, D. (2018). Investigation of Image Processing based Real-time Flood Monitoring. In *Measurement and Applications*.

Raja, N. S. M., Fernandes, S. L., Dey, N., Satapathy, S. C., & Rajinikanth, V. (2018). Contrast enhanced medical MRI evaluation using Tsallis entropy and region growing segmentation. *Journal of Ambient Intelligence and Humanized Computing 2018*, 1–12. https://doi.org/10.1007/S12652-018-0854-8.

Rao, K. R., & Ben-Arie, J. (1994). Optimal Edge Detection Using Expansion Matching and Restoration. *IEEE Transactions on Pattern Analysis and Machine Intelligence*, *16*(12), 1169–1182. https://doi.org/10.1109/34.387490.

Ratheash, R. S., &Sathik, M. M. (2013). Comparison of Segmentation based on Threshold and K-Means Method. *International Journal of Computer Science Trends and Technology (IJCST)*, *5*. www.ijcstjournal.org

Rezatofighi, H., Tsoi, N., Gwak, J., Sadeghian, A., Reid, I., & Savarese, S. (2019). *Generalized Intersection over Union: A Metric and A Loss for Bounding Box Regression*. http://arxiv.org/abs/1902.09630.

Robie, A. A., Seagraves, K. M., Egnor, S. E. R., Branson, K., Levine, J. D., Kronauer, D. J. C., & Dickinson, M. H. (2017). Machine vision methods for analyzing social interactions. *Journal of Experimental Biology*, *220*(1), 25–34. https://doi.org/10.1242/JEB.142281.

Ronneberger, O., Fischer, P., & Brox, T. (2015). U-net: Convolutional networks for biomedical image segmentation. *Lecture Notes in Computer Science (Including Subseries Lecture Notes in Artificial Intelligence and Lecture Notes in Bioinformatics)*, *9351*, 234–241. https://doi.org/10.1007/978-3-319-24574-4_28/COVER/.

Rudner, T. G. J., Rußwurm, M., Fil, J., Pelich, R., Bischke, † Benjamin, Kopačková, V., &BilíNski, P. (2019). Multi 3 Net: Segmenting Flooded Buildings via Fusion of Multiresolution, Multisensor, and Multitemporal Satellite Imagery. *The Thirty-Third AAAI Conference Artificial Intelligence (AAAI-19)*, 702–709. www.aaai.org.

Sadiq, A. A., Noor, K. I., & Nada, T. A. (2019). Satellite Images Segmentation Based on Histogram and Active Contour Algorithm. *Journal of Advanced Research in Dynamical & Control Systems,11*(02), 1–19. https://www.researchgate.net/publication/333004665.

Salvador, S., & Chan, P. (2004). Determining the number of clusters/segments in hierarchical clustering/segmentation algorithms. *Proceedings - International Conference on Tools with Artificial Intelligence, ICTAI*, 576–584. https://doi.org/10.1109/ICTAI.2004.50

Sathya, P., & Malathi, L. (2011). Classification and Segmentation in Satellite Imagery Using Back Propagation Algorithm of ANN and K-Means Algorithm. *International Journal of Machine Learning and Computing*, *4*(1), 422–426.

Schroff, F., Kalenichenko, D., & Philbin, J. (2015). FaceNet: A unified embedding for face recognition and clustering. *Proceedings of the IEEE Computer Society Conference on Computer Vision and Pattern Recognition*, *07-12-June*, 815–823. https://doi.org/10.1109/CVPR.2015.7298682

Seaberg, D., Devine, L., & Zhuang, J. (2017). A review of game theory applications in natural disaster management research. *Natural Hazards*, *89*(3), 1461–1483. https://doi.org/10.1007/S11069-017-3033-X.

Sebastian, R. V., Estefania, P. G., & Andres, O. D. (2020). Scalogram-energy based segmentation of surface electromyography signals from swallowing related muscles. *Computer Methods and Programs in Biomedicine*, *194*, 105480. https://doi.org/10.1016/J.CMPB.2020.105480

Sharifzadeh, S., Tata, J., Sharifzadeh, H., & Tan, B. (2020). Farm area segmentation in satellite images using deeplabv3+ neural networks. *Communications in Computer and Information Science*, *1255 CCIS*, 115–135. https://doi.org/10.1007/978-3-030-54595-6_7.

Shi, J., & Malik, J. (2000). Normalized cuts and image segmentation. *IEEE Transactions on Pattern Analysis and Machine Intelligence*, *22*(8), 888–905. https://doi.org/10.1109/34.868688

Singh, J., & Kaur, H. (2019). Plant disease detection based on region-based segmentation and KNN classifier. *Lecture Notes in Computational Vision and Biomechanics*, *30*, 1667–1675. https://doi.org/10.1007/978-3-030-00665-5_154/COVER/

Soomro, S., Munir, A., & Choi, K. N. (2018b). Hybrid two-stage active contour method with region and edge information for intensity inhomogeneous image segmentation. *PLoS ONE*, *13*(1). https://doi.org/10.1371/journal.pone.0191827

SowparnikaB. (2014). Adaptive Thresholding in Ultrasonograph Images. *International Journal of Scientific & Engineering Research*, *5*(5). http://www.ijser.org

Srinivasulu, K., & Premkumar, ; S. (2021). Gradient Based Edge Detection of Traffic Image using Second Derivative Method Compared with First Derivative Method. *RevistaGeintec-GestaoInovacao E Tecnologias*, *11*(4), 1126–1137.

Strîmbu, V. F., & Strîmbu, B. M. (2015). A graph-based segmentation algorithm for tree crown extraction using airborne LiDAR data. *ISPRS Journal of Photogrammetry and Remote Sensing*, *104*, 30–43. https://doi.org/10.1016/j.isprsjprs.2015.01.018

Strom, J., Richardson, A., & Olson, E. (2010). Graph-based segmentation for colored 3D laser point clouds. *IEEE/RSJ 2010 International Conference on Intelligent*

*Robots and Systems, IROS 2010 - Conference Proceedings*, 2131–2136. https://doi.org/10.1109/IROS.2010.5650459

Su, L., Fu, X., Zhang, X., Cheng, X., Ma, Y., Gan, Y., & Hu, Q. (2018). Delineation of Carpal Bones from Hand X-Ray Images Through Prior Model, and Integration of Region-Based and Boundary-Based Segmentations. *IEEE Access*, *6*, 19993–20008. https://doi.org/10.1109/ACCESS.2018.2815031

Sun, W., Bocchini, P., & Davison, B. D. (2020). Applications of artificial intelligence for disaster management. *Natural Hazards 2020 103:3*, *103*(3), 2631–2689. https://doi.org/10.1007/S11069-020-04124-3

Suzuki, K. (2017). Overview of deep learning in medical imaging. *Radiological Physics and Technology 2017 10:3*, *10*(3), 257–273. https://doi.org/10.1007/S12194-017-0406-5

Teng, L., Li, H., Yin, S., Karim, S., & Sun, Y. (2019). An active contour model based on hybrid energy and fisher criterion for image segmentation. *International Journal of Image and Data Fusion*, *11*(1), 97–112. https://doi.org/10.1080/19479832.2019.1649309.

Tian, Y., Zhou, M. Q., Wu, Z. K., & Wang, X. C. (2009). A region-based active contour model for image segmentation. *CIS 2009 - 2009 International Conference on Computational Intelligence and Security*, *1*, 376–380. https://doi.org/10.1109/CIS.2009.238

Tiwari, A., Mishra, V. K., & Mishra, M. (2020). Real Time optimization for image using hybridized Filter and K-Means Clustering. *Print) International Research Journal of Management Science & Technology*, *11*(8), 38–46. http://www.irjmst.com

Tolias, Y. A., & Panas, S. M. (1998). A fuzzy vessel tracking algorithm for retinal images based on fuzzy clustering. *IEEE Transactions on Medical Imaging*, *17*(2), 263–273. https://doi.org/10.1109/42.700738

Udupa, J. K., LeBlanc, V. R., Zhuge, Y., Imielinska, C., Schmidt, H., Currie, L. M., Hirsch, B. E., & Woodburn, J. (2006). A framework for evaluating image segmentation algorithms. *Computerized Medical Imaging and Graphics*, *30*(2), 75–87. https://doi.org/10.1016/J.COMPMEDIMAG.2005.12.001

Ulmas, P., & Liiv, I. (2020). Segmentation of Satellite Imagery using U-Net Models for Land Cover Classification. *IEEE Access*, *4*. http://arxiv.org/abs/2003.02899

van Westen, C. (2000). Remote Sensing for Natural Disaster Management. *International Archives of Photogrammetry and Remote Sensing*, *33*(3), 1609–1617.

Vincent, O., & Folorunso, O. (2009). A Descriptive Algorithm for Sobel Image Edge Detection. *Proceedings of the 2009 InSITE Conference*. https://doi.org/10.28945/3351

Wang, J., Ju, L., & Wang, X. (2011). Image Segmentation Using Local Variation and Edge-Weighted Centroidal Voronoi Tessellations. *IEEE TRANSACTIONS ON IMAGE PROCESSING*, *20*(11). https://doi.org/10.1109/TIP.2011.2150237

Wang, W., Lai, Q., Fu, H., Shen, J., Ling, H., & Yang, R. (2022). Salient Object Detection in the Deep Learning Era: An In-Depth Survey. *IEEE Transactions on*

*Pattern Analysis and Machine Intelligence*, *44*(6), 3239–3259. https://doi.org/10.1109/TPAMI.2021.3051099

Wazarkar, S., Keshavamurthy, B. N., & Hussain, A. (2018). Region-based Segmentation of Social Images Using Soft KNN Algorithm. *Procedia Computer Science*, *125*, 93–98. https://doi.org/10.1016/J.PROCS.2017.12.014

Wong, Q. O., & Rajendran. Parvathy. (2019). Image Segmentation using Modified Region-Based Active Contour Model. *Journal of Engineering and Applied Sciences*, *14*(16), 5710–5718.

Wu, W., Chen, A. Y. C., Zhao, L., & Corso, J. J. (2013). Brain tumor detection and segmentation in a CRF (conditional random fields) framework with pixel-pairwise affinity and superpixel-level features. *International Journal of Computer Assisted Radiology and Surgery 2013 9:2*, *9*(2), 241–253. https://doi.org/10.1007/S11548-013-0922-7

Wu, X., Pan, H., Xu, M., Jing, Z., & Bao, M. (2021). A Unified Framework for Joint Moving Object Detection and Tracking in the Sky and Underwater. *Proceedings of the International Conference on Aerospace System Science and Engineering* , 211–224. https://doi.org/10.1007/978-981-16-8154-7_17.

Xiaohan, Y., Yla-Jailski, J., Huttunen, O., Vehkomiiki, T., Sipila, O., & Katila, T. (1992). *Image Segmentation Combining Region Growing and Edge Detection*.

Xu, S., Wang, R., Wang, H., & Yang, R. (2021). Plane Segmentation Based on the Optimal-Vector-Field in LiDAR Point Clouds. *IEEE Transactions on Pattern Analysis and Machine Intelligence*, *43*(11), 3991–4007. https://doi.org/10.1109/TPAMI.2020.2994935

Ye, E. Z., Ye, E. H., Bouthillier, M., & Ye, R. Z. (2022). DeepImageTranslator V2: analysis of multimodal medical images using semantic segmentation maps generated through deep learning. *BioRxiv*, 2021.10.12.464160. https://doi.org/10.1101/2021.10.12.464160

Ye, H., Ding, M., & Yan, S. (2018). Improved Edge Detection Algorithm of High-Resolution Remote Sensing Imagesbased on Fast Guided Filter. *IEEE 4th Information Technology and Mechatronics Engineering Conference*, 29–33.

Yi, F., & Moon, I. (2012). Image segmentation: A survey of graph-cut methods. *2012 International Conference on Systems and Informatics, ICSAI 2012*, 1936–1941. https://doi.org/10.1109/ICSAI.2012.6223428

Yi, Z., Yongliang, S., & Jun, Z. (2019). An improved tiny-yolov3 pedestrian detection algorithm. *Optik*, *183*, 17–23. https://doi.org/10.1016/J.IJLEO.2019.02.038

Yu, M., Yang, C., & Li, Y. (2018). Big Data in Natural Disaster Management: A Review. *Geosciences*, *8*(165), 1–26. https://doi.org/10.3390/geosciences8050165

Yuheng, S., & Hao, Y. (2017). *Image Segmentation Algorithms Overview*. ArXiv, abs/1707.02051 https://doi.org/10.48550/arXiv.1707.02051

Zaitoun, N. M., & Aqel, M. J. (2015). Survey on Image Segmentation Techniques. *Procedia Computer Science*, *65*, 797–806. https://doi.org/10.1016/J.PROCS.2015.09.027

Zeebaree, D. Q., Zeebaree, D. Q., Haron, H., Mohsin Abdulazeez, A., &Zeebaree, S. R. M. (2017). Combination of K-means clustering with Genetic Algorithm: A review. *International Journal of Applied Engineering Research*, *12*, 14238–14245. http://www.ripublication.com

Zhang, C., Li, G., Lin, G., Wu, Q., & Yao, R. (2021). CycleSegNet: Object Co-Segmentation with Cycle Refinement and Region Correspondence. *IEEE Transactions on Image Processing*, *30*, 5652–5664. https://doi.org/10.1109/TIP.2021.3087401

Zhang, K., Chen, J., Liu, B., & Liu, Q. (2020). Deep Object Co-Segmentation via Spatial-Semantic Network Modulation. *Proceedings of the AAAI Conference on Artificial Intelligence*, *34*(07), 12813–12820. https://doi.org/10.1609/AAAI.V34I07.6977

Zhang, M., Dong, B., & Li, Q. (2020). Deep Active Contour Network for Medical Image Segmentation. *Lecture Notes in Computer Science (Including Subseries Lecture Notes in Artificial Intelligence and Lecture Notes in Bioinformatics)*, *12264 LNCS*, 321–331. https://doi.org/10.1007/978-3-030-59719-1_32/COVER/

Zhang, S., Xie, Y., Wan, J., Xia, H., Li, S. Z., & Guo, G. (2020). WiderPerson: A Diverse Dataset for Dense Pedestrian Detection in the Wild. *IEEE Transactions on Multimedia*, *22*(2), 380–393. https://doi.org/10.1109/TMM.2019.2929005

Zhang, T., Lin, G., Liu, W., Cai, J., & Kot, A. (2020). Splitting Vs. Merging: Mining Object Regions with Discrepancy and Intersection Loss for Weakly Supervised Semantic Segmentation. *Lecture Notes in Computer Science (Including Subseries Lecture Notes in Artificial Intelligence and Lecture Notes in Bioinformatics)*, *12367 LNCS*, 663–679. https://doi.org/10.1007/978-3-030-58542-6_40/COVER/

Zhao, Z. Q., Zheng, P., Xu, S. T., & Wu, X. (2019). Object Detection with Deep Learning: A Review. *IEEE Transactions on Neural Networks and Learning Systems*, *30*(11), 3212–3232. https://doi.org/10.1109/TNNLS.2018.2876865

Zhou, S. K., Greenspan, H., Davatzikos, C., Duncan, J. S., van Ginneken, B., Madabhushi, A., Prince, J. L., Rueckert, D., & Summers, R. M. (2021). A Review of Deep Learning in Medical Imaging: Imaging Traits, Technology Trends, Case Studies with Progress Highlights, and Future Promises. *Proceedings of the IEEE*, *109*(5), 820–838. https://doi.org/10.1109/JPROC.2021.3054390

Zhou, Z., Xue-Chang, Z., Si-Ming, Z., Hua-Fei, X., & Yue-Ding, S. (2018). Semi-automatic Liver Segmentation in CT Images Through Intensity Separation and Region Growing. *Procedia Computer Science*, *131*, 220–225. https://doi.org/10.1016/J.PR OCS.2018.04.206

# APPENDIX

## SOURCE CODE

### Edge-based Active Contour (EAC) Code

```
A = imread('flood7.jpg');
I = rgb2gray(A);
figure
imshow(I)
title('Original Image')

mask = false(size(I));
mask(25:end-25,25:end-25) = true;
BW = activecontour(I, mask, 8000);
figure
imshow(BW)
title('contour Image')

%ground Truth Image
BW_groundTruth = imread('mask6.jpg');
BW_groundTruth = logical(BW_groundTruth);
figure
imshow(BW_groundTruth)
title('Ground Truth Image')

%Intersection-over-Union (IoU, Jaccard index)
similarity = jaccard(BW, BW_groundTruth);
figure
imshowpair(BW, BW_groundTruth)
title(['Jaccard Index = ' num2str(similarity)])

%Dice
similarity1 = dice(BW, BW_groundTruth);
```

```
figure
imshowpair(BW, BW_groundTruth)
title(['Dice Index = ' num2str(similarity1)])

%Contour Matching Score
[similarity2,precision,recall] = bfscore(BW, BW_groundTruth);
figure
imshowpair(BW, BW_groundTruth)
title(['BF Score = ' num2str(similarity2)])
```

**Colour Thresholding Code**

```
function [BW,maskedRGBImage] = createMask(RGB)
%createMask  Threshold RGB image using auto-generated code from colourThresholder app.
% [BW,MASKEDRGBIMAGE] = createMask(RGB) thresholds image RGB using
% auto-generated code from the colourThresholder app. The colourspace and
% range for each channel of the colourspace were set within the app. The
% segmentation mask is returned in BW, and a composite of the mask and
% original RGB images is returned in maskedRGBImage.
%----------------------------------------------------------------------
% Convert RGB image to chosen colour space
I = rgb2hsv(RGB);

% Define thresholds for channel 1 based on histogram settings
channel1Min = 0.025;
channel1Max = 0.075;

% Define thresholds for channel 2 based on histogram settings
channel2Min = 0.277;
channel2Max = 0.416;

% Define thresholds for channel 3 based on histogram settings
```

```
channel3Min = 0.565;
channel3Max = 0.702;

% Create mask based on chosen histogram thresholds
sliderBW = (I(:,:,1) >= channel1Min ) & (I(:,:,1) <= channel1Max) & ...
   (I(:,:,2) >= channel2Min ) & (I(:,:,2) <= channel2Max) & ...
   (I(:,:,3) >= channel3Min ) & (I(:,:,3) <= channel3Max);
BW = sliderBW;

% Initialize output masked image based on input image.
maskedRGBImage = RGB;

% Set background pixels where BW is false to zero.
maskedRGBImage(repmat(~BW,[1 1 3])) = 0;
end
```

**Region-based Active Contour (RAC) code**

```
function [BW,maskedImage] = segmentImage(RGB)
%segmentImage Segment image using auto-generated code from imageSegmenter app
% [BW,MASKEDIMAGE] = segmentImage(RGB) segments image RGB using
% auto-generated code from the imageSegmenter app. The final segmentation
% is returned in BW, and a masked image is returned in MASKEDIMAGE.
 %------------------------------
% Convert RGB image into L*a*b* colour space.
X = rgb2lab(RGB);
% Create empty mask.
BW = false(size(X,1),size(X,2));

% Draw Freehand
xPos = [69.1917 69.7390];
yPos = [18.7379 19.2852];
m = size(BW, 1);
```

```
n = size(BW, 2);
addedRegion = poly2mask(xPos, yPos, m, n);
BW = BW | addedRegion;

% Active contour
iterations = 600;
BW = activecontour(X, BW, iterations, 'Chan-Vese');

% Create masked image.
maskedImage = RGB;
maskedImage(repmat(~BW,[1 1 3])) = 0;
end
```

**K-means Clustering Code**

```
% Load image
img = imread('flood2.jpg');

% Convert image to grayscale
gray_img = rgb2gray(img);

% Convert image to double precision
double_img = im2double(gray_img);

% Define number of clusters
num_clusters = 3;

% Perform k-means clustering
[cluster_idx, cluster_center] = kmeans(double_img(:), num_clusters);

% Reshape cluster indices to match image size
cluster_img = reshape(cluster_idx, size(double_img));
```

```
% Convert cluster indices to uint8 format
cluster_img = uint8(cluster_img);

% Display original image and segmented image side-by-side
figure;
subplot(1,2,1);
imshow(gray_img);
title('Original Image');
subplot(1,2,2);
imshow(cluster_img);
title('Segmented Image');
```

**Colour-based k-means Clustering Code**

```
clc;clear;
he = imread('flood7.jpg');
figure; imshow(he)

lab_he = rgb2lab(he);
figure; imshow(lab_he)

ab = lab_he(:,:,2:3);
nrows = size(ab,1);
ncols = size(ab,2);
ab = reshape(ab,nrows*ncols,2);
nColours = 3;
% repeat the clustering 3 times to avoid local minima
[cluster_idx, cluster_center] = kmeans(ab,nColours,'distance','sqEuclidean', ...
                                       'Replicates',3);
pixel_labels = reshape(cluster_idx,nrows,ncols);

segmented_images = cell(1,3);
rgb_label = repmat(pixel_labels,[1 1 3]);
```

```
for k = 1:nColours
    colour = he;
    colour(rgb_label ~= k) = 0;
    segmented_images{k} = colour;
end
figure
imshow(segmented_images{1}), title('objects in cluster 1');
figure
imshow(segmented_images{2}), title('objects in cluster 2');
figure
imshow(segmented_images{3}), title('objects in cluster 3');
diseases = segmented_images{1};
figure
imshow(diseases);
gray_scale = rgb2gray(diseases);
b = imadjust(gray_scale);
BW = imbinarize(b);
BW2 = imfill(BW,'holes');
figure; imshow(BW2);
```